Quaternary Science Reviews 30 (2011) 280–297

Contents lists available at ScienceDirect

Quaternary Science Reviews

journal homepage: www.elsevier.com/locate/quascirev

Vegetation response to obliquity and precession forcing during the Mid-Pleistocene Transition in Western Mediterranean region (ODP site 976)

Sébastien Joannin [a,b,*], Franck Bassinot [c], Nathalie Combourieu Nebout [c], Odile Peyron [a], Célia Beaudouin [d]

[a] CNRS-USR 3124 MSHE Ledoux/CNRS-UMR 6249 LCE, 32 rue Mégevand, 25030 Besançon, France
[b] CNRS-UMR 5125 PEPS, Université de Lyon, 69622 Lyon, France
[c] LSCE-UMR 8212 CNRS/CEA/UVSQ, Domaine du CNRS, Bat.12, Avenue de la terrasse, 91198 Gif sur Yvette Cedex, France
[d] TOTAL, Avenue Larribau, 64018 Pau Cedex, France

ARTICLE INFO

Article history:
Received 21 July 2009
Received in revised form
26 October 2010
Accepted 11 November 2010
Available online 8 December 2010

ABSTRACT

The ODP leg 161 Site 976 (Alboran Sea) is a deep-sea section sampled at a water depth of 1108 m in the Western Mediterranean Sea. Pollen analysis provides a vegetation and climate record of the Mid Pleistocene Transition (MPT), roughly one million years ago. The age-model tied to biostratigraphic events was revised by aligning the pollen climate index (PCI) to Mediterranean (KC01b) and global (LR04) oxygen isotope records. The studied time slice spans the interval ~1.09 Ma (MIS 31) to ~0.90 Ma (MIS 23).

Across this interval, past phytogeography of nowadays extinct taxa, which were rare, allows a successful application of the modern analogues technique (MAT) to quantitative climate reconstructions for the MPT. Five, long-term, obliquity-related vegetation successions (O1 to O5), and eight short-term, precession-related vegetation successions (P1 to P8) are observed within the studied interval. These vegetation successions, regardless of their duration, show the same pattern: the progressive replacement of temperate trees by mountainous taxa, and then by herbs and steppe maxima. Precession-related successions correspond, therefore, to as dramatic vegetation changes as those driven by obliquity, including a final steppe phase under deteriorated climate conditions.

Wavelet analysis of the PCI record shows that the Western Mediterranean experienced a shift at 1.01 Ma from precession-dominated frequencies (1.05–1.01 Ma) to obliquity-dominated frequencies (1.01–0.9 Ma). There is, therefore, an apparent discrepancy between wavelet analysis results and vegetation dynamic analysis (which suggests that obliquity and precession are recorded throughout the entire studied interval). This discrepancy could result from the fact that the PCI record sums, somehow, similar vegetation changes (wet to dry) occurring at different periodicities. Such a complex vegetation dynamics is mathematically rendered through a single parameter (i.e. principal component), which does not successfully catch the subtle combinations of variability occurring at two close periodicities. Furthermore, the pollen-inferred Early Pleistocene vegetation dynamic (and climate) of the Western Mediterranean region does not show a decrease of the obliquity response relative to the precession response at the onset of the MPT.

1. Introduction

During Pliocene and Pleistocene times, Earth climate was affected by a progressive, long-term cooling over which 10^4–105 yr climate cycles were superimposed (e.g. Ruddiman, 2003; Lisiecki and Raymo, 2007). Those global climatic variations were dominated by 41 kyr-long oscillations during the Early Pleistocene, as a climate system response to the obliquity orbital parameter forcing. About 1 Ma ago, during the Early–Middle Pleistocene, the response of the global climatic system shifted and showed the progressive dominance of an eccentricity and precession combination, resulting in the appearance of 100 kyr-long cycles (Von Grafenstein et al., 1999; Ruddiman, 2003). This shift from the earlier "41 kyr world" to the subsequent "100 kyr world" corresponds to a period of increased cooling called the Mid Pleistocene Transition. The first authors to really focus on it, suggested that this transition period lasted about 250 kyr, from ~0.90 Ma to 0.65 Ma (Berger and Jansen, 1994; Mudelsee and Stattegger, 1997), corresponding to the onset of the first important glaciations (MIS 22–24), and to the subsequent increase in the 100 kyr oscillation. Yet, more recent works clearly suggest that this transition period could actually start earlier and last longer, spanning the time interval from 1.2 Ma to 0.5 Ma (Head and Gibbard, 2005).

* Corresponding author. CNRS-UMR 5125 PEPS, Université de Lyon, 69622 Lyon, France. Tel.: +33 3 81 66 62 58; fax: +33 3 81 66 65 68.
E-mail addresses: sebastien.joannin@mshe.univ-fcomte.fr (S. Joannin), Franck.Bassinot@lsce.ipsl.fr (F. Bassinot), Nathalie.Nebout@lsce.ipsl.fr (N.C. Nebout), odile.peyron@univ-fcomte.fr (O. Peyron), celia.beaudouin@total.com (C. Beaudouin).

0277-3791/$ – see front matter © 2010 Elsevier Ltd. All rights reserved.
doi:10.1016/j.quascirev.2010.11.009

Cyclic changes in the obliquity of the Earth's axis has a profound effect on the seasonal insolation at high latitudes (Berger and Loutre, 2004), but has a minute effect on climate variability at low latitudes (Liu and Herbert, 2004). An opposite feature characterizes the precession influence, which is dominant at low latitudes (Ruddiman and McIntyre, 1984; Shackleton et al., 1999; Maslin and Ridgwell, 2005).

Oxygen isotope measurements in benthic foraminifera are a proxy for global ice volume and deep-water temperature changes in response to orbital variations (Raymo and Nisancioglu, 2003). For times before the MPT, Raymo et al. (2006) observed that ocean $\delta^{18}O$ or sea-level proxies recorded the dominant obliquity (41 kyr) component of insolation, while 23 and 19 kyr changes (the precession signature) were not expressed. The MPT marks a shift to "in-phase" behavior of northern and southern ice sheets as well as the strengthening of 23 kyr cyclicity in the marine $\delta^{18}O$ record (Raymo et al., 2006). However, the MPT is usually described through spectral analysis or band-pass filtering, and the "bifurcation" to the new mode of the climatic system is not easy to see from raw data (Maslin and Ridgwell, 2005). The MPT is a transitional period during which cycles of non-Milankovitch periods can be observed (e.g. Maslin and Ridgwell, 2005).

Because of the Mediterranean Sea geographical position (between 30 and 42 °N *senso stricto*), we expect that climate proxies embedded in Mediterranean sediments have recorded the influence of both obliquity and precession (Kroon et al., 1998). Not only does the Mediterranean Sea spread over a large latitudinal domain, but [1] it has a much larger catchment area that drains waters (eventually pollen grains) from 20 °N up to 47 °N, and [2] its wind system extends beyond this area. As for the other areas of the world ocean, the $\delta^{18}O$ of Mediterranean deep waters, recorded in benthic foraminifera, is dominated by the so-called global isotopic signal related to waxing and waning of continental ice caps (Ruddiman, 2003), and shows the transition from 41 kyr-dominant to the 100-kyr dominant oscillations at the MPT. This global, benthic $\delta^{18}O$ signal is the backbone of the marine isotopic stratigraphy. On the other hand, regional climate changes are largely dominated by precession in the Mediterranean region. Precession drives, for instance, changes in wetness (precipitation/evaporation) and, therefore, sea-surface salinity that result in $\delta^{18}O$ fluctuations recorded by surface-dwelling planktonic foraminifera (Emeis et al., 2003). During Northern Hemisphere summer insolation maxima, when precession is minimal, those precession-controlled changes in precipitation can lead to the drastic decrease in Mediterranean Sea-surface salinity, the subsequent reduction in deep-water ventilation and the resulting formation of sapropels (Rohling and Hilgen, 1991). In the eastern Mediterranean area, Kroon et al. (1998) indicate that the apparition and strengthening of the long 100 kyr cycle is associated with a reinforced precession influence during and after the MPT. Yet, surprisingly, despite numerous evidence of precession influence on Mediterranean paleo-sedimentation, stable oxygen isotope records from ODP sites 976 and 977 have revealed a weak precessional component in Pleistocene records from the Alboran Sea (Von Grafenstein et al., 1999).

Pollen analysis can be successfully used to reconstruct climate changes, which occurred during the Northern Hemisphere glacial–interglacial cycles in the Mediterranean area (Wijmstra and Smit, 1976; Suc and Zagwijn, 1983; Suc, 1984; Combourieu Nebout and Vergnaud Grazzini, 1991; Ravazzi and Rossignol-Strick, 1995; Tzedakis and Bennett, 1995; Subally et al., 1999; Joannin et al., 2007a) and, more particularly, during the MPT (Russo Ermolli, 1994; Moscariello et al., 2000; Okuda et al., 2002; Capraro et al., 2005; Ravazzi et al., 2005; Tzedakis et al., 2006; Joannin, 2007; Joannin et al., 2007b, 2008, 2010). However, so far, quantitative climate reconstructions based on pollen assemblages older than the Upper Pleistocene were only attempted for Miocene and Pliocene climatic changes in the Mediterranean area (e.g. Fauquette et al., 1998; Klotz et al., 2006; Jiménez-Moreno et al., 2010). All these records provided information on Tertiary inherited taxa disappearance related to reinforced climatic cycles and to the long-term, global cooling (i.e. Svenning, 2003; Tzedakis et al., 2006; Rohais et al., 2007) with a special focus on Italian taxa replacement (Bertini et al., 2010; Magri, 2010; Follieri, 2010; Fusco, 2010; Magri et al., 2010). However, they remain restricted to the Central and Eastern Mediterranean regions.

In the Western Mediterranean region (Iberian Peninsula), no pollen studies were devoted to the MPT. Few pollen records focused on older climate cycles (Rio Maior: Diniz, 1984; Suc et al., 1995a; Tres Pins: Leroy, 1997). Over the last 2.6 Ma (Quaternary), the rapid glacial–interglacial fluctuations are well marked in climate reconstructions where they mostly correspond to temperature changes while variations in precipitation were seemingly rapid through this period and precipitation reached very low values (Jiménez-Moreno et al., 2010). Most of the pollen records, on the contrary, focused to the very last climate cycles (ODP Site 976: Combourieu Nebout et al., 1999, 2002; core MD95-2043: Sánchez-Goñi et al., 2002; Fletcher and Sánchez-Goñi, 2008; Fletcher et al., 2010).

Vegetation succession is an ecological term that usually designs a progressive vegetation replacement through time. It takes place after a catastrophic disruption of an ecosystem and can be applied in paleoecology, at an interglacial onset, for instance (Birks and Birks, 2004). Long-term ecosystem evolution records a phase of ecological development with increasing productivity and nutrient availability, followed by a retrogressive phase with the decline of these parameters. In Northern Europe, edaphic conditions play a major role in this succession, however, their influence have been questioned for the Southern Europe (Tzedakis and Bennett, 1995). Long-term vegetation successions related to glacial–interglacial changes have been observed in European pollen sequences (e.g. Ioannina, Tzedakis and Bennett, 1995; Velay, De Beaulieu et al., 2006). In the Mediterranean area, pollen-based spectral analyses have shown that in addition to ~100 kyr glacial/interglacial climatic cycles, vegetation successions also record precession and obliquity variations during the late Pliocene and Pleistocene times (e.g. Tenaghi Philippon, Mommersteeg et al., 1995; Tzedakis et al., 2006; Crotone series, Klotz et al., 2006). If vegetation successions can reasonably be linked to climate cycles through temperature and precipitation changes, it is not clear how insolation changes in the precession and obliquity bands initiated and/or forced the course of vegetation change. Interactions between precession and obliquity forcings are quite difficult to unravel. Regarding the sapropel formation in the Mediterranean Sea, for instance, Lourens et al. (1996) suggested that obliquity and precession effects can sometimes add up and sometimes act in opposite directions. Large-scale processes such as conditions leading to sapropel formation must have affected the vegetation around the Mediterranean basin. Joannin et al. (2007a) visually linked vegetation successions and orbital parameters. However, so far, no study has tried to couple visual and spectral approaches together on a high resolution and long enough pollen section to study accurately the respective effects of precession and obliquity on the vegetation evolution across the MPT.

We obtained a new pollen record from ODP Site 976, covering the beginning of the MPT (1.09–0.90 Ma). The series was sampled at a resolution appropriate to resolve Milankovitch-related oscillations, changes in pollen assemblages, thus, accurately document vegetation replacements that resulted from regional and global climate changes. We were particularly interested to look at the precession effects (Joannin et al., 2007a) in a geographic context (mid latitudes) where obliquity has a strong impact on long-term changes in seasonal distribution of insolation. For that purpose, the ODP Site 976 record

appeared particularly suitable since planktonic $\delta^{18}O$ was already available (Von Grafenstein et al., 1999) as well as reconstructed SST (González-Donoso et al., 2000), providing a preliminary stratigraphy as well as a background of regional marine variability to which pollen assemblage changes could be compared. The orbitally-forced climatic changes embedded in our high-resolution pollen record also allow to refine the ODP Site 976 age-model over the studied interval. Our study makes it possible, for the first time, [1] to provide the pollen-inferred past phytogeography and to reconstruct quantitatively climate parameters for the south-western Mediterranean region over the MPT, and [2] to analyze vegetation successions in the time domain and in the frequency domain, by combining the "classical" pollen analysis approach with powerful signal processing tools (i.e. wavelet analysis) in order to better understand the vegetation response to climate change and insolation forcing.

2. General setting of site 976 core

2.1. Core location and sedimentation

The ODP Site 976 (36°12.3′N, 4°18.8′W; leg 161) is a deep-sea section sampled at a water depth of 1108 m in the western Alboran Sea (Fig. 1). It is located at ~45 km off the southern Spanish coast, ~150 km off the northern Moroccan coast and ~110 km east of the Strait of Gibraltar. The 346 m-long hemipelagic sedimentary section provides an almost complete Pliocene and Pleistocene record of climatic and oceanographic variability in the western Mediterranean Sea. During the coring, partial loss of sediment occurred between 190–197 and 284–287 mcd. The high sedimentation rate estimated for the entire sedimentary section (0.23 m/kyr) reflects the delivery of sediments to this site by a combination of repetitive turbidity events and settling of pelagic sediments (Bernasconi et al., 1999), leading to the alternation of turbidite mud layers embedded in hemipelagic mud. Over the studied interval (i.e. ~260 to ~230 mcd), turbidites are considered as low-energy (end-products) gravity-flows that originate from the margin, mainly through the Fuengirola Canyon (Alonso et al., 1999). Sediments contain ~47% of clay minerals, ~19% of quartz, ~29% of calcite and <5% of dolomite. The clay assemblage is constituted of detrital clays (~62% of illite, ~10% of kaolinite and ~14% of chlorite) and ~14% of smectites (Martínez-Ruíz et al., 1999).

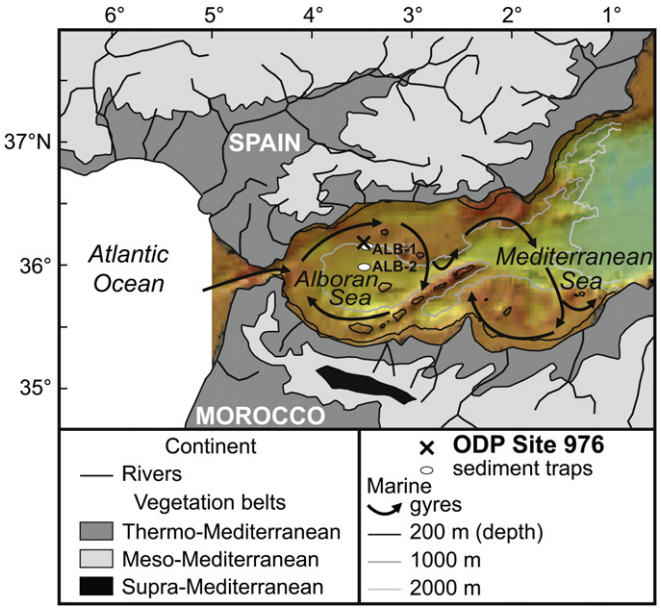

Fig. 1. ODP site 976 (this study) and sediment traps (Fabrés et al., 2002) location in the Alboran Sea.

2.2. Stratigraphy and age-models

Von Grafenstein et al. (1999) obtained a $\delta^{18}O$ curve of the planktonic foraminifera *Globigerina bulloides*. They used this record to identify the marine isotopic stages (MIS) and to develop an age-model. De Kaenel et al. (1999) provided nannofossil analyses coupled with sapropelic stratigraphy (using orbital tuning from Lourens et al., 1996) to establish nannofossil event ages. González-Donoso et al. (2000) estimated winter and summer SST from foraminifer assemblages. They made an attempt to correlate those SST variations with insolation changes across the entire Quaternary. Significant mismatches exist between the SST-derived and the $\delta^{18}O$-derived age-models of Site 976 within the MPT (González-Donoso et al., 2000), and particularly in the interval studied in the present work (i.e. ~260 to ~230 mcd). Inconsistencies between these two independent age-models can either result from the low-resolution of the $\delta^{18}O$ record and/or from the fact that only some well-dated nannofossil events were used to constrain the SST-based age-model (see González-Donoso et al., 2000). An important aspect of the present work will be to improve the ODP Site 976 age-model over the MPT interval.

3. Material and methods

3.1. Pollen analysis

Seventy-nine samples have been collected at ~40 cm intervals from 259.50 to 230.42 mcd. Samples were processed using a standard method adapted from Cour (1974). HCl and HF treatments were followed by sievings at 160 μm and 10 μm and by a final enrichment procedure ($ZnCl_2$). Only fifty-nine samples provided enough pollen grains (150 grains excluding *Pinus*) for reliable analysis. Thus, about 14 000 pollen grains were counted in the studied section. A rich pollen flora of 70 taxa was documented in our analyses (at least 20 taxa per sample), including arboreal together with herbaceous plants, which live today over a large range of latitudes (Fig. 2). *Pinus* pollen grains are overrepresented in marine deposits (Heusser, 1988; Beaudouin et al., 2007). Consequently, taxa percentages were calculated with respect to the total pollen grains sum minus the *Pinus* contribution, while *Pinus* abundance was normalized to the total pollen sum. The detailed pollen diagram (Fig. 2) presents arboreal and herbs and shrubs taxa classified from base to top and grouped according to the ecology of their representatives in the present-day plant ecosystems (Suc, 1984; Combourieu Nebout, 1987).

To simplify the visualisation of the pollen signal, we performed a Principal Component Analysis (PCA) using PAST (PAleontological Statistic) program (Hammer et al., 2001). It provides an unscaled pollen index (see 4.1. Pollen analysis for more details; Fig. 2) roughly corresponding to climate variations and used to determine pollen phases. We labelled these phases A to F, from the older one to the most recent.

3.2. Pollen-based climate reconstruction

The Modern Analogues Technique (MAT: Hutson, 1980; Guiot, 1990) is usually applied to reconstruct climate changes in Mediterranean area during younger periods, for example during the Eemian (Brewer et al., 2008), the Lateglacial and the Holocene (e.g. Davis et al., 2003; Cheddadi et al., 2005; Kotthoff et al., 2008; Davis and Brewer, 2009; Combourieu Nebout et al., 2009; Dormoy et al., 2009; Peyron et al., in press). Applications of this method to Mid Pleistocene and older pollen sequences are very rare (Plio-Pleistocene climate in

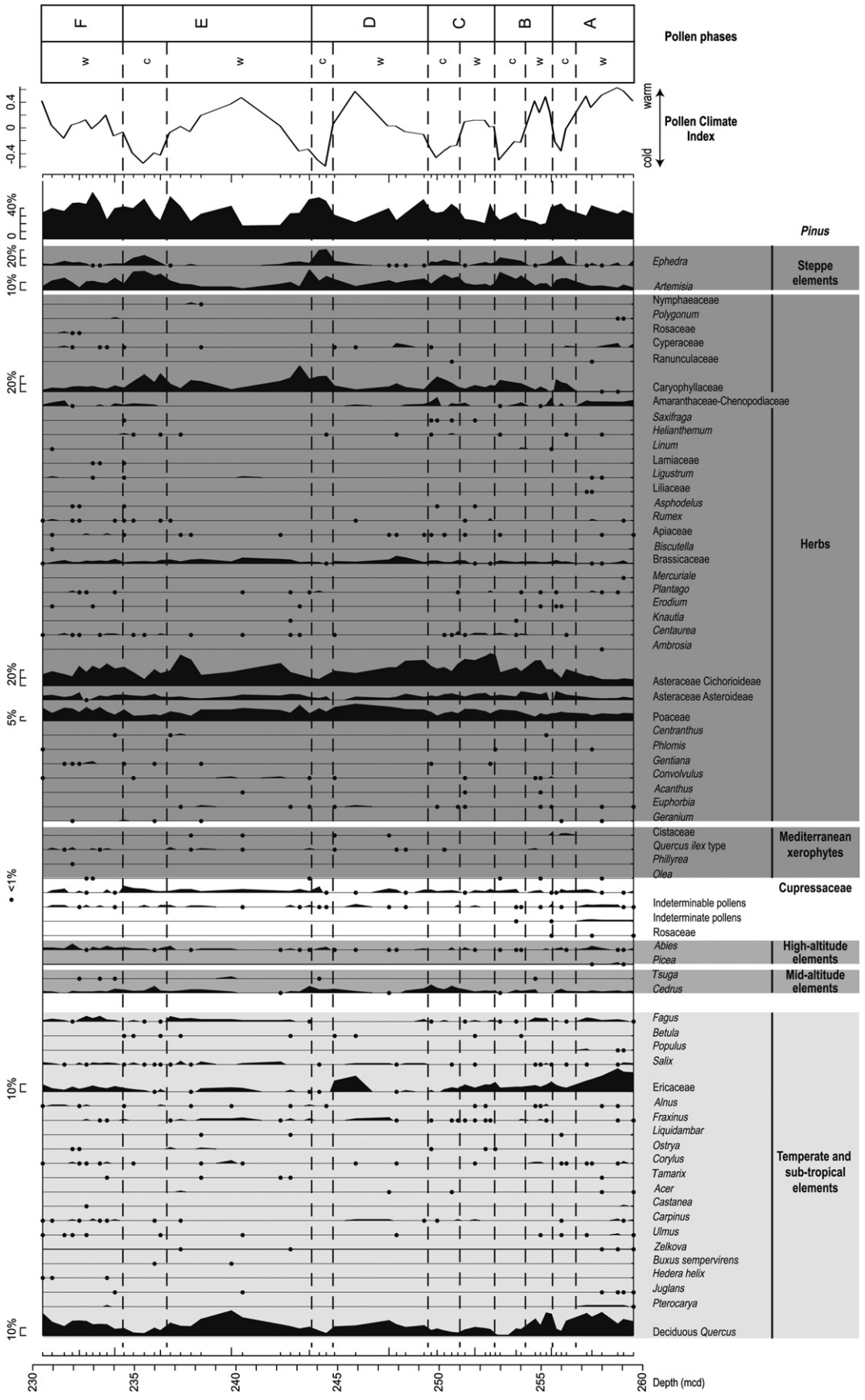

Fig. 2. Detailed pollen diagram of ODP Site 976 from ~260 mcd to ~230 mcd. All taxa (except *Pinus*) are represented in relative percentages, which are calculated based on the total of counted pollen grains minus *Pinus*. Only *Pinus* has a relative percentage based on the total of counted pollen grains. Vegetation groups are based on the ecological significance of their present-day representatives: temperate and sub-tropical elements (such as deciduous *Quercus*, Ericaceae…), mid-altitude elements (*Cedrus*, *Tsuga*), high-altitude elements (*Picea*, *Abies*), Mediterranean xerophytes (such as *Olea*), herbs (such as Poaceae, Asteraceae Asteroideae…) and steppe elements (such as *Artemisia* and *Ephedra*). On the right, the pollen climate index (PCI) allows to discriminate pollen phases (stratigraphically noted A to F from base to top) that include alternation of warm "w" and cold "c" phases.

Africa; Bonnefille et al., 2004) because of the occurrence of subtropical Tertiary inherited taxa leading to situations where no modern analogues are available. For Miocene and Pliocene periods, mutual climatic range methods such as the 'climatic amplitude method' developed by Fauquette et al. (1998) or the "probability mutual climatic spheres" (Klotz et al., 2006) seem to be more appropriate because these methods are able to reconstruct the climate changes when no analogue exists in the modern pollen floras (Jiménez-Moreno et al., 2010). In the ODP 976 pollen assemblages, the Tertiary inherited taxa (*Liquidambar*, *Zelkova*, *Pterocarya* and *Tsuga*) are very rare, and their percentages are very low (Fig. 2), so they could be excluded by the MAT. Thus, these taxa have not been taken into account in the climatic reconstruction. In the present work, the MAT is based on a modern pollen dataset that contains more than 3500 modern spectra with 2000 samples from the Mediterranean area (Dormoy et al., 2009). Since *Pinus* is overrepresented in marine sediments, this pollen grain has been removed from the marine pollen counting used for quantitative climate reconstruction as well as from the continental pollen database (e.g. Combourieu Nebout et al., 2009). The similarity between each fossil sample and modern pollen assemblages is evaluated by a chord distance (Guiot, 1990). Usually, a selection of 8–10 modern spectra that have the smallest distance provides robust modern analogues of the given pollen spectrum and are subsequently used for the reconstruction. Quantitative climate reconstructions for ODP Site 976 focused on summer and winter temperature and precipitation changes. Annual temperature and precipitation have also been estimated since these parameters seem to be key parameters in the Ericaceae distribution of the Iberian Peninsula (Ojeda et al., 1998).

3.3. Spectral and wavelet analysis

There exist several spectral analysis methods. Among them, the Maximum Entropy Method (MEM) produces high-resolution power spectra. This inverse method solves for autoregressive model parameters (the power spectra are not forced into the parametric mold of a Fourier series). MEM is a precise spectral tool but has a tendency to yield spurious peaks and shows a reduced resolution in the presence of noise. These weaknesses are usually remedied by comparing, for instance, MEM spectra to those produced using other spectral methods, such as the Blackman-Tukey approach (BT; which should not share spurious peaks with MEM). There, BT record similar frequencies. Prior to spectral analyses, in order to get an evenly sampled dataset, PCI values have been re-sampled using a simple (60 samples), cubic spline function with an interpolated 3.14 kyr resolution (*Analyseries* software, version 1.05; Paillard et al., 1996). Then MEM analyses were carried out with the *Strati-Signal* free software (version 1.0.5, University of Geneva; Ndiaye, 2007), using the Durbin-Levinson algorithm with a number of lags of 30.

The periodograms obtained through either the MEM or the Blackman-Tukey techniques give spectral power distributions versus frequencies. They do not provide pieces of information about potential spectral evolution through time. To obtain a time-frequency representation of a non-stationary, periodic signal one has to use wavelet transform approaches. In order to check potential changes in dominant frequencies through time embedded in our ODP Site 976 proxy series, we performed wavelet analyses using the *Strati-Signal* software.

4. Results

4.1. Pollen analysis

It is generally assumed that pollen mostly come from rivers in marine detrital deposits (Heusser, 1988; Cambon et al., 1997). It is also the case for turbiditic sediments even if the sedimentary pathway from the river to the turbidites is more complex (Beaudouin et al., 2004). In marine pelagic environments such as in the Gulf of Guinea, it has been shown that pollen grains are wind-transported (Hooghiemstra et al., 2006). Let us look at the elements in hands that allow deciphering between an eolian and a fluvial origin for pollen grains at Site ODP 976. The percentage of dinoflagellate cysts can give us an indication about the main transportation mode of the pollen grains (Beaudouin et al., 2004). Dinoflagellate cysts are produced in the photic zone. They are mixed with eolian particles such as pollen grains during the decantation process. When wind transport prevails, the relative contribution of oceanic dinoflagellate cysts to sedimentary biogenic material is much more important than that of the pollen grains (De Vernal, 2009). This explains that in pelagic environment such as in present-day sediment deposited at 2326 m of water depth in the Gulf of Lions, the palynological assemblage contains up to 70% of dinoflagellate cysts (Beaudouin et al., 2004), whereas this contribution drops to 25% maximum on the shelf (Beaudouin et al., 2007) where fluvial inputs dominate (Aloisi, 1986). In the ODP Site 976, dinoflagellate cysts constitute 24% on average of the total palynomorphs counted, suggesting that wind transportation of pollens does not dominate here. In two sediment traps (ALB-1, 36°1'N, 4°16'W, 1004 m; ALB-2, 36°01'N, 4°18'W, 1337 m; Fig. 1) very close to the ODP Site 976, the material retrieved corresponds predominantly to lithogenic particulate material (68–76%; Fabrés et al., 2002). Fluxes suggest that, today, eolian inputs of lithogenic material probably play only a limited role since average dust fluxes recorded in Granada are one order of magnitude lower than the lithogenic fluxes recorded in both trap locations. Yet, clays and palynomorphs found at ODP Site 976 were interpreted as a mix of both detritic and pelagic sedimentation sources (Bout-Roumazeilles et al., 2007). This conclusion is confirmed by the fact that we found few reworked grains in our samples contrary to other regions were detrital sedimentation is dominant (Beaudouin et al., 2007). So, today, elements in hands suggest that in the vicinity of ODP Site 976, we deal with a mixed pollen assemblage in which the fluvial contribution is more important that the wind contribution. In both cases, whether they are river- or wind-transported, pollen grains are representative of the vegetation belts encountered in drainage basins or the adjacent continent, respectively (Beaudouin et al., 2005; Hooghiemstra et al., 2006).

Our results reveal a rich and diversified pollen flora (Fig. 2) with herbs, Mediterranean xerophytes (*Olea*, *Quercus ilex*, Cistaceae…), mesothermic (i.e. warm-temperate) and mid-altitude taxa (deciduous *Quercus*, Betulaceae, Juglandaceae, Salicaceae, Ulmaceae, Fagaceae, Pinaceae Abietoideae…).Our samples contain taxa found in the Early and Middle Pleistocene of the Mediterranean region, such as *Liquidambar*, *Zelkova* and *Pterocarya* (mesothermic elements), and *Cedrus* and *Tsuga* (mid-altitude elements). Combourieu Nebout et al. (1999) and Sánchez-Goñi et al. (2002) observed high amounts of *Cedrus* pollen grains (up to 60% and 20%, respectively) in the Middle and Upper Pleistocene marine sediments from the same area. In our samples, *Cedrus* is not as abundant since it reaches only 10% at the maximum. The Ericaceae abundance (6.4% on average) shows a particular outline that recalls the typical pattern of the Ericaceae widespread in the Western Mediterranean region from the Early Zanclean (Rio Maior: Diniz, 1984; Suc et al., 1995a) to the Holocene (Naughton et al., 2007). High amounts of Asteraceae Cichorioideae (20.8% on average) are found in the ODP Site 976, as in the older lacustrine sediments from Tres Pins borehole (Northeastern Spain: Leroy, 1997).

4.2. Pollen climate index (PCI)

For Middle Pleistocene sediments from the same ODP Site, Combourieu Nebout et al. (1999) related mesothermic elements

maxima to interglacials, and steppe elements maxima with *Pinus* to glacials. The present data show a pronounced opposition between mesothermic and steppe elements ($r = -0.69$; $p < 0.001$). The first (principal) Factor obtained through the PCA analysis explains 35% of the data variance (available as a QSR Online Background Dataset) and rests upon a strong opposition between ecological groups: mesothermic elements, on the one hand, and Caryophyllaceae, Amaranthaceae–Chenopodiaceae and steppe elements, on the other hand. These members are unambiguously anti-correlated ($r = -0.75$; $p < 0.001$). The first Factor discriminates, therefore, [1] pollen phases characterized by a relative increase of the mesothermic group (i.e. forest) that indicates warm-temperate and wet conditions, from [2] pollen phases characterized by the decrease of the mesothermic pollen contribution and the relative increase of herb pollen grains (i.e. herbs and steppes), which indicate cold and dry conditions. Thus, we have labelled the former phases "w" (warm) and the later "c" (cold), respectively. We have grouped each warm-temperate phase ("w") with the corresponding colder phase ("c") that follows it stratigraphically. There are five complete "w–c" doublets in the interval studied (A to F). Thus, the first Factor provides us with a pollen climate index (PCI). Unfortunately, phases Dw and Ew have a poor time-resolution, as only a few samples obtained in these intervals contained enough pollen grains for meaningful assemblage analyses. However, the high percentage of mesothermic elements obtained in all the samples available from these two phases (>30% of the pollen sum excluding *Pinus*) strongly supports the idea that no major colder or drier phase could have been missed within Dw and Ew.

5. Discussion

5.1. Stratigraphy and age-model

5.1.1. $\delta^{18}O$- and SST-based stratigraphies

In the upper part of the studied interval, the stratigraphic assignment of MIS 23–27 based on Site 976 planktonic $\delta^{18}O$ record (Von Grafenstein et al., 1999) is coherent with the stratigraphic scheme deduced from the SST record (González-Donoso et al., 2000; Fig. 3). The isotopic stratigraphy, down to MIS 27, is also coherent with biostratigraphy datums (Table 1). As expected, the first occurrence (FO) of *Gephyrocapsa omega* (>4 μm), that takes place between 244.03 and 243.75 mcd, occurs at the MIS 26–25 transition, and the last common occurrence (LCO) of *Reticulofenestra asanoi*, found at 229.91 mcd, occurs during the MIS 23–22 transition (Real and Menochi, 2005). In the lower part of the studied interval (i.e. 260–230 mcd), however, the poor resolution of the $\delta^{18}O$ record and the low amplitude of the fluctuations recorded make it difficult to recognise unambiguously the MIS. The inferred-MIS 28 in the $\delta^{18}O$ record appears, for instance, as a poorly defined peak, and cold SST temperatures recorded over this stratigraphic interval are rather invariant. Surprisingly also, higher SST winter temperatures are recorded during the $\delta^{18}O$-derived MIS 30 than during the following interglacial MIS 29. The rather poor correlation that exists between the $\delta^{18}O$ and SST records results in two different stratigraphic schemes for this interval (Von Grafenstein et al., 1999; González-Donoso et al., 2000). The ambiguities about the stratigraphy are such that the work from De Kaenel et al. (1999) suggests that our studied interval starts within the interglacial MIS 31, whereas the work from González-Donoso et al. (2000) indicates that it starts within the glacial MIS 30.

5.1.2. A revised ODP site 976 stratigraphy

To circumvent the relatively poor quality of the $\delta^{18}O$ record and solve the discrepancies between the $\delta^{18}O$-derived and SST-derived stratigraphies, we propose to use the pollen climate index (PCI) as an additional, stratigraphic tool (Fig. 4). We used two isotopic

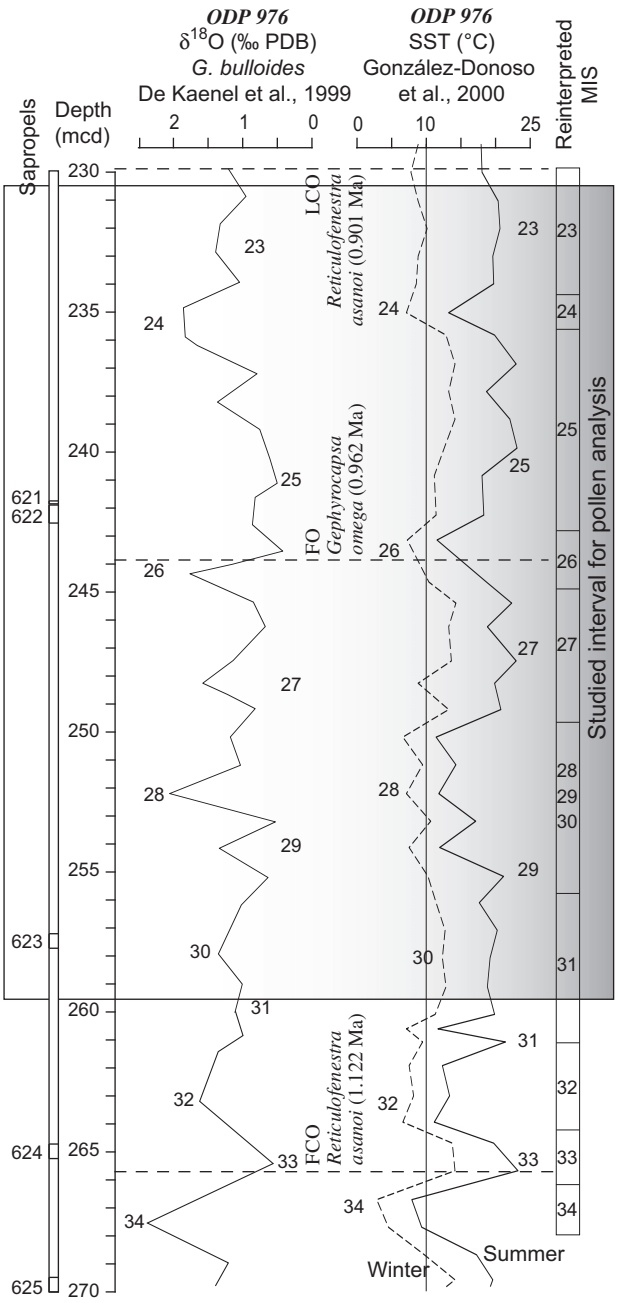

Fig. 3. The studied interval includes two sapropelic layers 622–621 (~242 mcd) and 623 (~257 mcd). Recently, Real and Menochi (2005) placed the FO of *Gephyrocapsa omega* between 244.03 and 243.75 mcd. Planktonic $\delta^{18}O$ record (De Kaenel et al., 1999) is compared with winter and summer SST records (González-Donoso et al., 2000). The $\delta^{18}O$-derived and SST-derived stratigraphies differ for this interval.

records as climatic "reference" curves: [1] a regional, planktonic (*Globigerinoides ruber*) oxygen isotope record from the Ionian Sea (KC01b; Rossignol-Strick and Paterne, 1999), and [2] the global, LR04 benthic oxygen isotope stack (Lisiecki and Raymo, 2005). The upper part of our studied interval, for which the stratigraphy seems to be robust, allows us to look at the relationships between the different proxies. It makes it possible, therefore, to set up and validate the combination of $\delta^{18}O$, SST, PCI and biostratigraphic datums as an integrated stratigraphic approach for the entire MPT interval in Site ODP 976.

The top of the studied interval is chronologically constrained by LCO of *R. asanoi*. The warm pollen phases Ew and Fw, characterized

Table 1
The eleven control points used to establish the chronostratigraphic framework of the studied interval: astronomically-calibrated nannofossil events (Real and Menochi, 2005), sapropels correlated with insolation cycles (*i*; Lourens, 2004) and five marine isotope stage (MIS) transitions used as tie-points.

Event	Depth (mcd)	Age (Ka)
Sapropel	620	(*i*-80) 220 841
MIS	22–21	Transition 224 868
LCO[a]	*R*	*Asanoi* 229.91 901
MIS	24–23	Transition 234.65 917
FO[b]	*G*	*Omega* 243.75 963
MIS	28–27a	Transition 249.35 1001
MIS	30–29	Transition 252.67 1032
Sapropel	623	(*i*-100) 257.5 1070
MIS	32–31	Transition 260.5 1090
FCO[c]	*R*	*Asanoi* 265.67 1122
Sapropel	625	(*i*-108) 269.74 1144

[a] LCO = last common occurrence.
[b] FO = first occurrence.
[c] FCO = first common occurrence.

by an increase in mesothermic elements, correspond to MIS 25 and MIS 23. Cold pollen phases Dc and Ec, characterized by a high percentage of steppe elements, clearly correspond to glacial MIS 26 and MIS 24 (the glacial MIS 26 being coevals to the *Gephyrocapsa omega* FO). Yet, the foraminifer-derived summer SST minimum (~243 mcd) is slightly offset from the glacial MIS 26 inferred from the $\delta^{18}O$ curve, while the interval of low PCI values (Dc) encompasses both the SST and $\delta^{18}O$ changes associated with MIS 26. In the middle part of the studied section, pollen phase Dw shows a double peak pattern (from ~245 to ~247.5 mcd and ~249 mcd), which is also recorded in the oxygen isotope and winter SST curves. This double peak that occurs during Dw can be related to the MIS 27 double peak (a and b). Clearly, therefore, in the upper part of the studied interval, the PCI record is strongly coherent with climatic oscillations inferred from the marine $\delta^{18}O$ and SST records.

Let us now discuss the stratigraphy of the lower, problematic part of the studied interval. If one looks beyond it (Fig. 3), both the $\delta^{18}O$ and the SST records appear to be coherent and to record MIS 34, 33 and 32. Such stratigraphic attributions are confirmed by the *R. asanoi* first common occurrence (FCO; Table 1) dated at 1.122 Ma and contemporaneous with the MIS 34–33 transition. As a result, the decreasing oxygen isotope values and the increasing temperatures, which are simultaneously recorded at ~261 mcd, likely correspond to the MIS 31 onset. This conclusion is in good accordance with the work from De Kaenel et al. (1999). This is also corroborated by the spectacular high amount of arboreal pollen (~70%) during pollen phase Aw, which suggests a long warm and humid episode. Warm conditions, however, are not clearly expressed in ODP Site 976 $\delta^{18}O$ record. This is likely a local signature and/or reflects the poor resolution of the ODP Site 976 record since MIS 31 does show up as strongly depleted $\delta^{18}O$

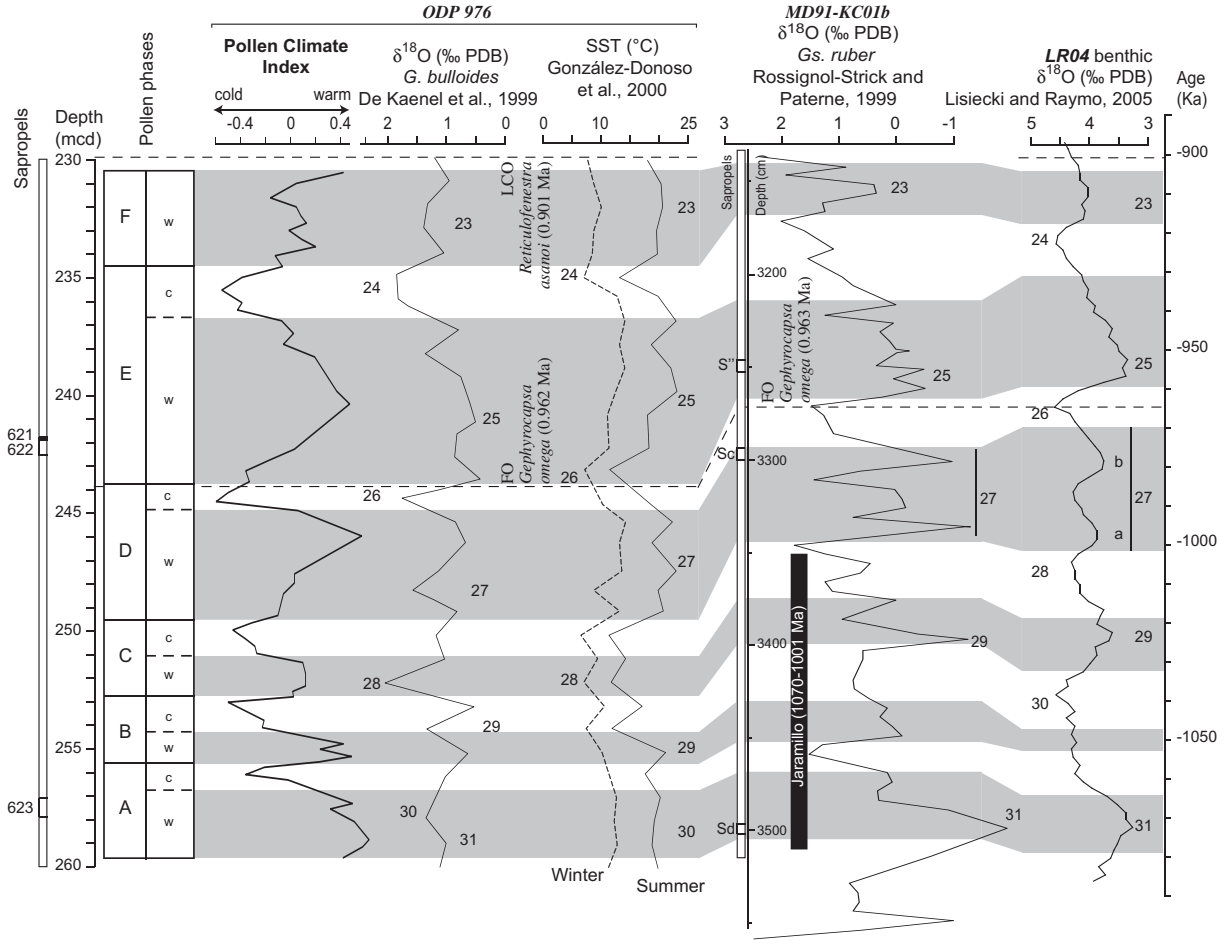

Fig. 4. To solve the discrepancies between the $\delta^{18}O$-derived and SST-derived stratigraphies, PCI and the warm-temperate pollen phases (grey shapes) are compared with two climatic "reference" curves: [1] a regional, planktonic oxygen isotope record from the Ionian Sea (KC01b; Rossignol-Strick and Paterne, 1999), and [2] the global, LR04 benthic oxygen isotope stack (Lisiecki and Raymo, 2005).

values in the KC01b record from the Ionian Sea. These long, warm and humid conditions during MIS 31 are also corroborated by pollen records from Southern Italy (Montalbano Jonico section; Joannin et al., 2008) and Greece (Tenaghi Philippon; Tzedakis et al., 2006). Consequently, the sapropel 623 which was previously associated with *i*-98 by De Kaenel et al. (1999) would be older.

If we are correct about MIS 31, then assuming a continuous record and a steady sedimentation rate implies that the Bw stage in the PCI record cannot be associated with MIS 29 [as would be the case if we used the stratigraphies developed by De Kaenel et al. (1999) or González-Donoso et al. (2000)]. Indeed, considering that Bw corresponds to MIS 29 would lead to an anomalously low sedimentation rate of ~0.063 m/kyr for the lower part of the studied interval (much lower than the sedimentation rate of ~0.185 m/kyr estimated over the MIS 27–23 interval). Tzedakis (2007) show that AP high values ran continuously for about 50 kyr (i.e. from ~1.090 to ~1.040 Ma) in Tenaghi Philippon while the *Quercus* percentages record several variations, one being related to an inner oscillation of the glacial MIS 30. Pollen phase Bw correlates with a $\delta^{18}O$ decrease and an SST increase. It can therefore be considered as a MIS 30 inner oscillation. Such an internal oscillation is observed in the $\delta^{18}O$ record from Ionian core KC01b. Thus, finally, pollen phase Cw appears to be associated with MIS 29, although there exists a phase-lag with regard to $\delta^{18}O$ and SST changes.

Despite the low-temporal resolution of the pollen record during the warm intervals related to mesothermic forest development (Dw and Ew), every Early Pleistocene climatic cycles (MIS 31 to MIS 23) can be identified. Pollen phases Aw, Cw, Dw, Ew and Fw are related to MIS 31, MIS 29, MIS 27 (bi-phased), MIS 25 and 23, respectively. The pollen phase Bw corresponds to isotopic depletions in ODP Site 976 and KC01b records. This occurs during the glacial MIS 30. In the lowermost part of the section, the correspondence between marine and vegetation records is less obvious, probably because of differences in sampling resolution, which make it difficult to correlate the records (i.e. 59, 33 and 30 samples in the pollen, isotope and SST analyses, respectively over the 30 m-long interval).

5.1.3. Age-model

In order to establish the most consistent age-model for the studied interval (i.e. ~260 to ~230 mcd; Fig. 5), we also took into account dated stratigraphic events located above and below (from 220 mcd, down to ~270 mcd). Eleven control points were used to develop the age-model (Table 1). Among these control points, we used three, astronomically-calibrated nannofossil events (Real and Menochi, 2005). In addition, sapropels 620, 621–622, 623 and 625 have been identified in Site ODP 976 and correlated with insolation cycles 80, 90, 100 and 108, respectively (Lourens, 2004). Finally, five MIS transitions were used as tie-points to accurately constrain the age-model (i.e. MIS 22–21, MIS 24–23, MIS 28–27a, MIS 30–29 and MIS 32–31). Thus, at the difference of the pollen record from Tenaghi Philippon Site which needed to be age-calibrated by assuming marine and terrestrial events synchronicity (Tzedakis et al., 2006), the present pollen record is directly dated with respect to astronomically-calibrated, marine stratigraphic events analyzed from the same samples making it possible to directly link marine and continental events. Between these control points, discrete samples were dated using a fourth order polynomial equation fitted over the tie-points from the 220–270 mcd interval. The studied interval covers ~190 kyr (from 1.090 to 0.90 Ma). On the whole, the age-model indicates a rather constant sediment accumulation rate, with a mean value of 0.157 m/kyr (Fig. 5). ODP 976 climatic interpretation is based on an average pollen temporal resolution of ~3200 years (59 samples covering ~190 kyr).

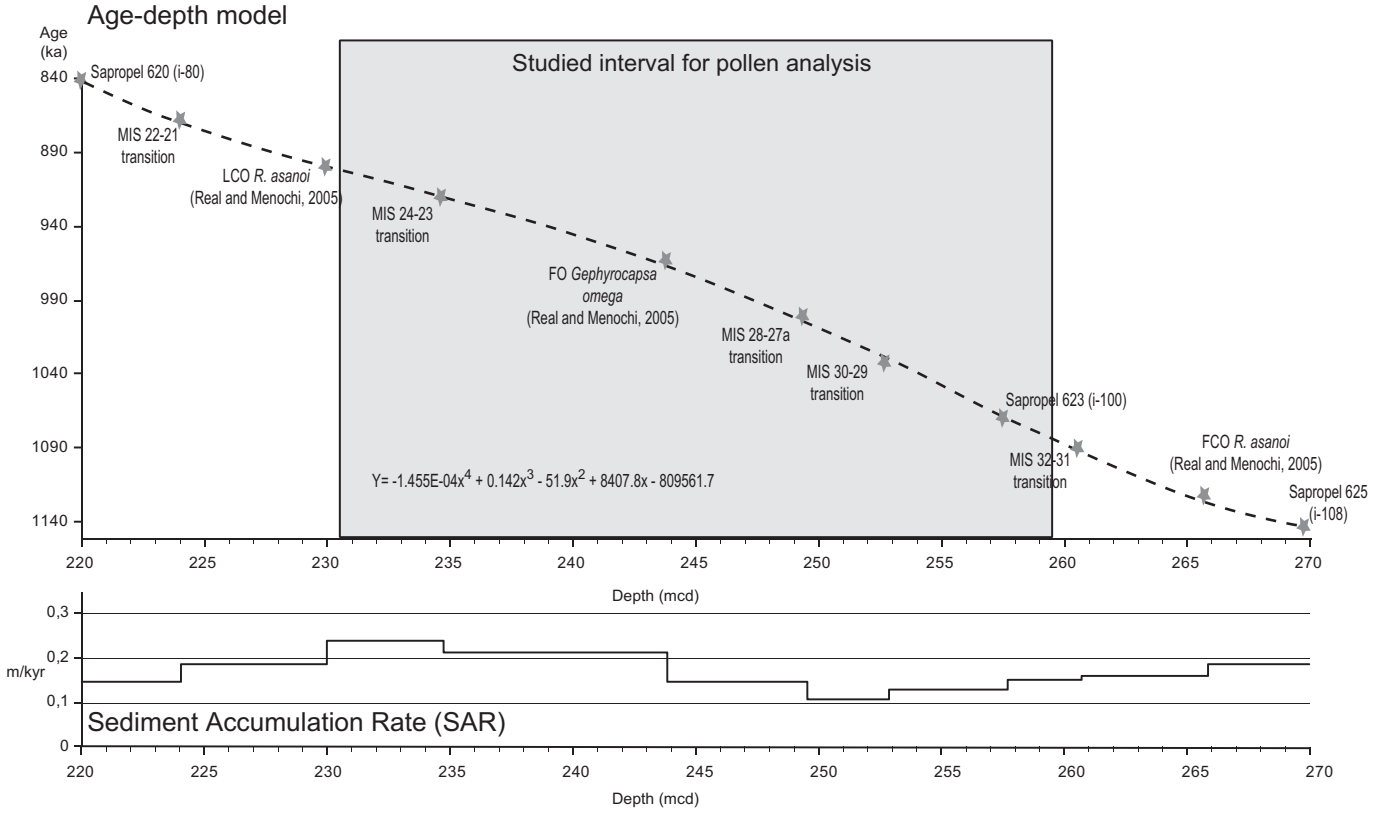

Fig. 5. Eleven datums (grey stars) are compiled from ~220 to ~270 mcd (see Table 1 and the associated caption for details) and placed on the age-model in order to build a regression equation (dashed line) and calculate ages of samples. The resulting sediment accumulation rate (SAR) is presented in meters per thousand years.

5.2. Pollen-inferred vegetation and climate reconstruction

5.2.1. Past phytogeography of nowadays extinct taxa

Cathaya, Taxodiaceae and *Carya* were not found in the pollen assemblage from the Early Pleistocene of ODP Site 976 (Fig. 3). Today, *Cathaya* inhabits the mid-altitude belt (ca 1200 m) in sub-tropical China, Taxodiaceae are broadly mega-mesothermic, and *Carya* is a mesothermic deciduous tree. All require warm and humid conditions and were present over the relief of southern Spain during the upper Pliocene (Jiménez-Moreno et al., 2010). During the lower to middle Pleistocene, they were present in Southern Italy (Montalbano Jonico section; Joannin et al., 2008). Thus, their absence in our pollen data should result from less favourable climatic conditions in the south-western part of the Mediterranean region. Our pollen assemblage shows that, *Pterocarya*, *Zelkova*, *Liquidambar*, and *Tsuga* were still present in the western Mediterranean region during the Early Pleistocene. *Pterocarya* and *Zelkova* develop during MIS 31, which is a long warm and humid interglacial, as attested in reconstructed precipitation (Fig. 6), that temporarily favoured expansion of taxa inherited from the sub-tropical Pliocene climate (Joannin et al., 2008). Early Pleistocene climatic conditions experienced a steady decrease in temperature and wetness as indicated by the absence of sub-tropical taxa such as *Cathaya*, Taxodiaceae and *Carya*. Moreover, *Pterocarya* and *Zelkova* rarefy in the following interglacials. This probably announces their imminent extinction in southern Iberia. The interglacial MIS 31 appears to be an exceptional period, with particularly warm conditions in the Mediterranean area. During the late Early Pleistocene, the transition from a warm and humid climate to a more temperate and drier climate is also confirmed by a paleontological study of small vertebrates in the nearby Guadix-Baza basin (Agustí et al., 2010). More generally, a broadly similar taxa disappearance scenario has been established in Italy (Bertini et al., 2010). Thus, we suggest that extinction in the western Mediterranean precedes extinction in the central Mediterranean area. This indicates an earlier deterioration of climate conditions that became less favourable for Tertiary inherited plants.

5.2.2. Past phytogeography of modern taxa

Thermophilous plants such as deciduous *Quercus* and Ericaceae require more than 600 mm of annual precipitation (Sánchez-Goñi et al., 2000). These plants mainly characterized warm and humid conditions corresponding to interglacials (i.e. odd-numbered MIS) of the Western Mediterranean region (Fig. 7a and b). Such a climatic signature already existed during the Pliocene in the region (Suc et al., 1995a). The *Quercus* pollen dominance is also observed during the Late Pleistocene warm intervals from the Alboran Sea (Sánchez-Goñi et al., 2002; Combourieu Nebout et al., 2002). Ericaceae document the oceanic influence (Sánchez-Goñi et al., 1999). Based on Iberian margin cores, Tzedakis et al. (2004) observed that heathland development occurred in both glacial and temperate phases. In ODP Site 976, however, the pollen record indicates the development of heathland during interglacial periods only., while it mostly characterized interglacial periods at ODP 976.Other taxa such as *Salix*, *Fraxinus*, *Carpinus* typify interglacials. Caryophyllaceae, Amaranthaceae–Chenopodiaceae and steppe elements may express xeric conditions associated with a large range in temperature (Subally and Quézel, 2002). They are correlated with glacial MIS in ODP Site 976 record and, therefore, associated with low sea-level episodes that created saline and arid environments in littoral areas of the Alboran Sea (Fig. 1). More generally, these new lands may offer good environmental conditions for opportunistic and heliophylous taxa like herbs and steppe elements. As a consequence, their development, which is enhanced by dry and cold climate, is possibly reinforced by newly available lands (Suc et al., 1995b; Joannin et al., 2008). Repeated increases in altitude-related taxa are observed, mainly *Cedrus*, which became more abundant during the warm to cold climate transitions. This conifer presently grows in a cool and humid climate between 1300 and 2600 m in the Rif, Middle Atlas and High Atlas mountains (Northern Africa; Cheddadi et al., 1998). Magri and Parra (2002) suggest that *Cedrus* pollen is of northwest African provenance and are brought, therefore, in pollen records from southwest Europe by winds blowing from Africa. Sánchez-Goñi et al. (1999) and Bout-Roumazeilles et al. (2007) proposed that *Cedrus* pollen grains were brought by southern Saharan winds into the Late Pleistocene sediments from Alboran Sea and Iberian margin (Atlantic side). However, considering the confirmed past extent of *Cedrus* trees in Europe and Southern Europe during Pliocene and Pleistocene, *Cedrus* pollen is expected to be supplied by the mid-altitude vegetation belt of southern Spain and northern Africa over the time interval studied in ODP Site 976.

5.2.3. Pollen-inferred climate reconstruction

Quantitative climate reconstructions in the Alboran Sea mimic the five distinct climate alternations recorded by the PCI between 1.09 and 0.9 Ma (Fig. 6). These reconstructions reveal higher temperatures and precipitation during interglacials as compared to the present-day climate while during the glacial phases, conditions were colder and dryer than today. The pollen phases Ac, Bc, Cc, Dc, Ec are characterized by a temperature and precipitation decrease, with particularly low temperature ($-10\,^{\circ}C$) during the youngest phases Dc and Ec while Ac, Bc and Cc are limited to $-5\,^{\circ}C$ and $-3\,^{\circ}C$, respectively. Temperatures of the coldest month during the glacial phases Dc and Ec are about 5 °C colder than the estimates obtained for the last glacial maximum from the same core by the same method (Bout-Roumazeilles et al., 2007). Those exceptionally low temperatures correspond to steppic pollen assemblages that are similar to those observed in sediments deposited during late Pleistocene Heinrich events (Bout-Roumazeilles et al., 2007). Estimated coldest month temperatures are systematically lower than current values for the Alboran Sea region even during the warm phases. Combourieu Nebout et al. (2009) already pointed out an underestimation of the winter temperatures values by about $-6\,^{\circ}C$. Taking this bias into account, observed winter temperature anomalies of about $-5\,^{\circ}C$ for older cold phases (Ac, Bc and Cc), fit well with -5 to $-7\,^{\circ}C$ reconstructed values for the glacial phases occurring from 2.6 to 1.75 Ma in northeastern Spain (Fauquette et al., 1998). In the Klotz et al. (2006) study, a mutual climatic range method applied to the Mediterranean marine pollen record of Semaforo (Italy) yielded detailed information about summer, annual and winter temperatures and on precipitation from ~2.46 to ~2.11 Ma. It showed that glacial phase temperatures are generally 5 °C lower than the present-day mean temperature in the region. Such cold temperatures are in good agreement with climatic estimates for MIS 30 and 28 glacial phases in the Alboran Sea. It is not clear whether the reconstructed $-10\,^{\circ}C$ cooling for the following cold phases Dc and Ec indicates deteriorated climate conditions for MIS 26 and 24 or a methodological bias due to the lack of modern analogues coming from high-elevation areas of Iran and Turkey. The global $\delta^{18}O$ record (LR04) clearly suggests an extension of polar ice sheet and/or colder high latitude temperatures during MIS 26 and 24. However, at least two modern pollen analogues, which are located in Inner Mongolia, induce very cold reconstructed values.

During the MPT, the pollen-based precipitation curve and the winter precipitation curve fit particularly well with the PCI and reconstructed SST values. Fig. 6 suggests two distinct periods of precipitation changes: [1] a period before 1 Ma with low winter and annual precipitations, and [2] the following interval, characterized by a trend towards a more marked cyclicity (phases D, E and F) with dry glacial phases and wetter than today interglacials. Before 1.05 Ma, the pollen-based climate reconstruction indicates that climate was wetter than today but anomalously cool (annual and warmest month) for an interglacial phase. Such a reconstruction is probably

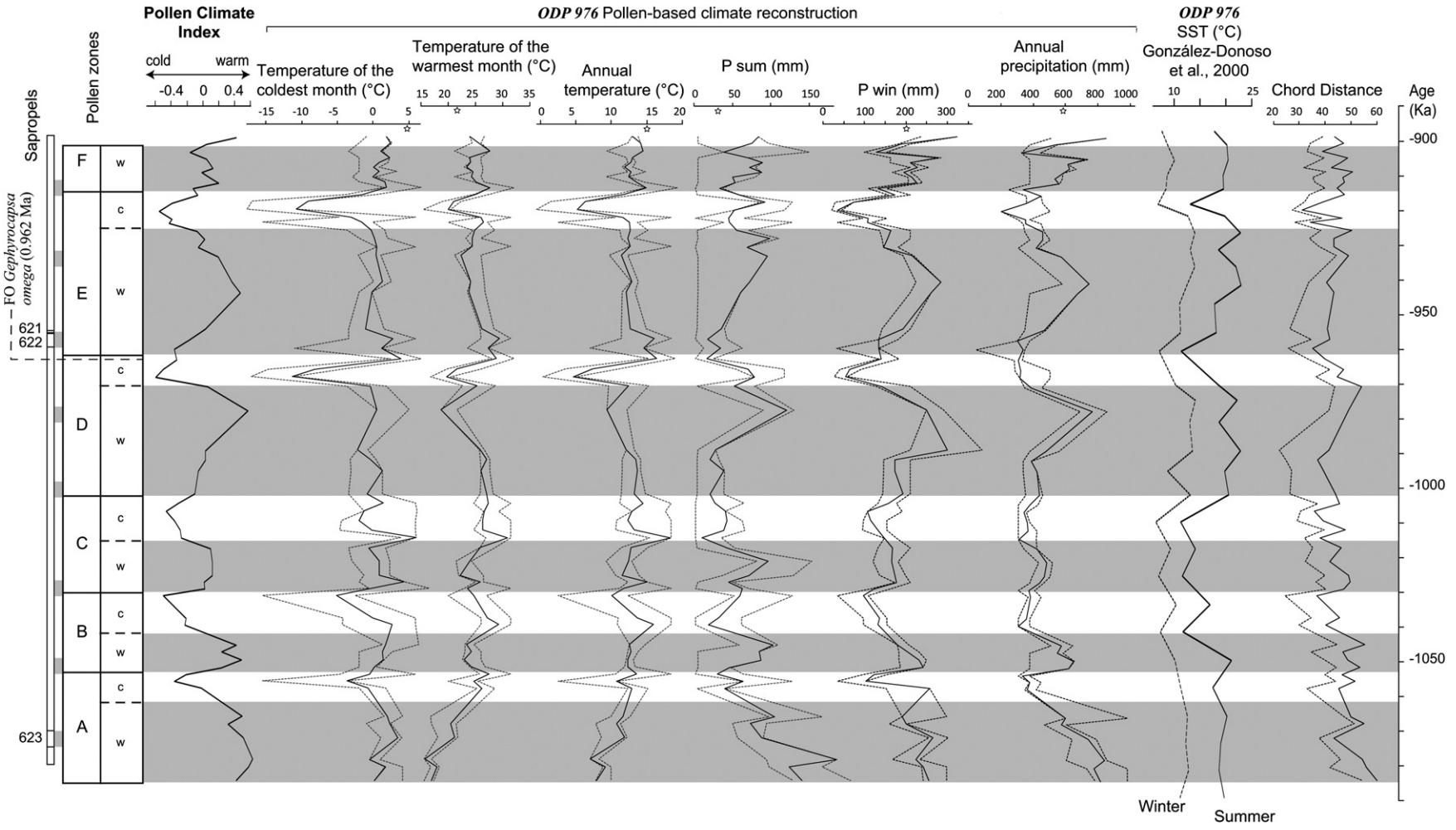

Fig. 6. Pollen-based climate reconstructions for ODP site 976. Climate values have been estimated using the Modern Analogues Technique (MAT). Temperatures of the coldest month and warmest month in °C are plotted together with summer and winter precipitation. Annual temperatures and precipitations are also plotted in age. Modern values are indicated with crosses. Climate estimates are compared with the independent SST reconstructed values, and with the pollen climate index.

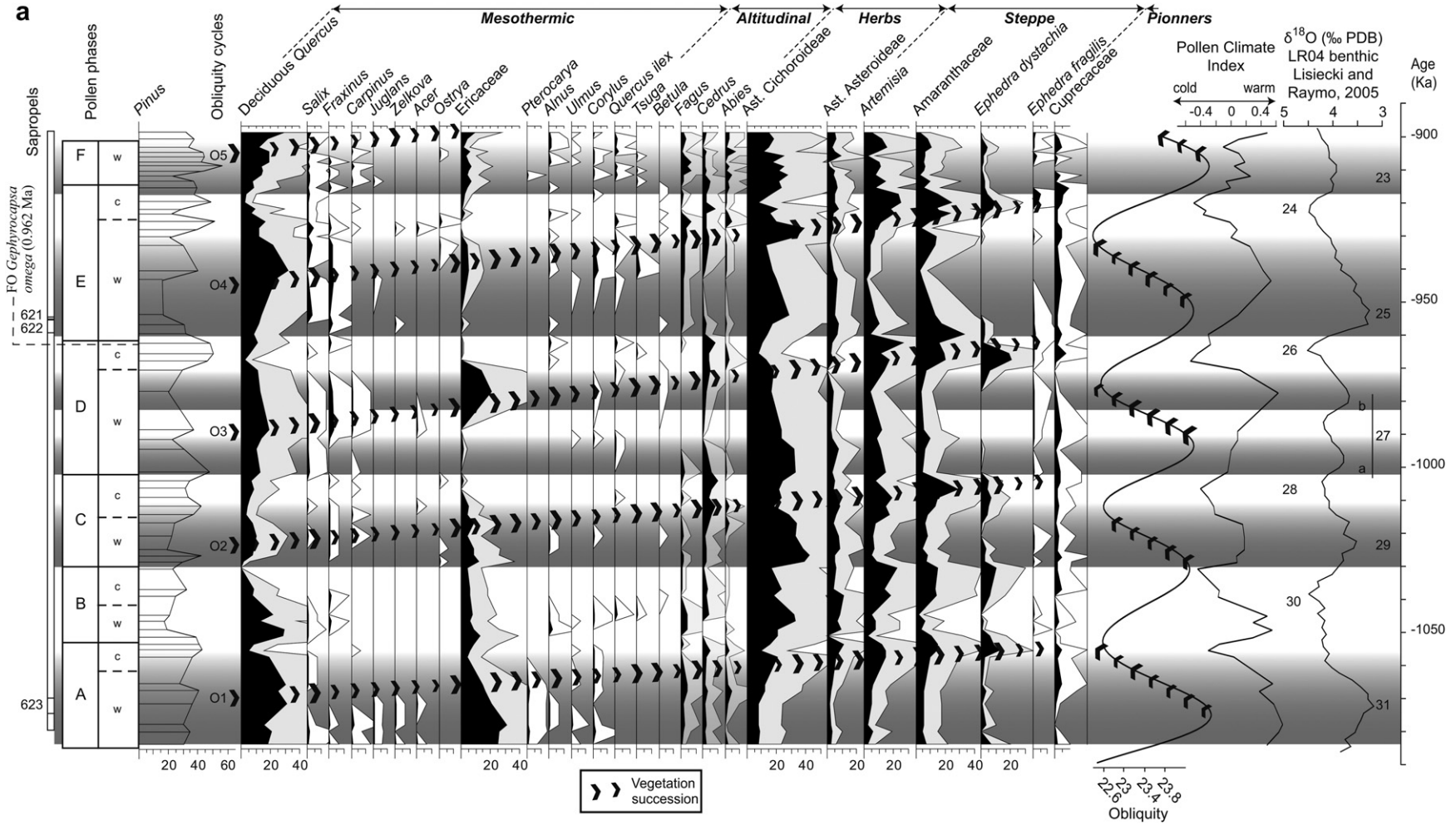

Fig. 7. a. Sapropels, pollen phases and nannofossil event, main pollen taxa percentages (based on total pollen except *Pinus*), pollen climate index, obliquity variations as well as oxygen isotope curve LR04 are presented in age. 4 complete and 1 incomplete vegetation successions illustrated by chevrons (noted O1–O5) are observed. Successions broadly show a similar pattern characterized by successive dominance of temperate trees (mainly *Quercus* deciduous and Ericaceae) followed by altitude elements (*Cedrus*, *Fagus*, *Abies*), and ending with herbs and steppe maxima (Ast. Cichorioideae, Amaranthaceae, *Artemisia*, *Ephedra dystachia*). Successions O1–O5 are reported by chevrons and correlate with obliquity shift from maxima to minima. They characterized vegetation and climate response to obliquity variation. 7b. Eight short-lived (P1–P8) vegetation successions are reported by using dotted lines. They are superimposed on the five long-lived (O1–O5) successions described in Fig. 7a and Table 2. These eight successions which are organized with the same pattern, can only be discriminate by their time-duration. As P1–P8 characterized the pollen-inferred vegetation response to precession variations, these successions are considered short-lived compared to those related to obliquity. Precession influence interpretation is reinforced by sapropel deposits that correlate with precession minima (grey bars). Moreover, pollen climate index maxima precisely follows the eccentricity curve. Since insolation is mainly forced by precession, which is modulated in terms of amplitude by 100 kyr eccentricity (Lisiecki, 2010), climate and vegetation changes observed in the ODP Site 976 also record an eccentricity component.

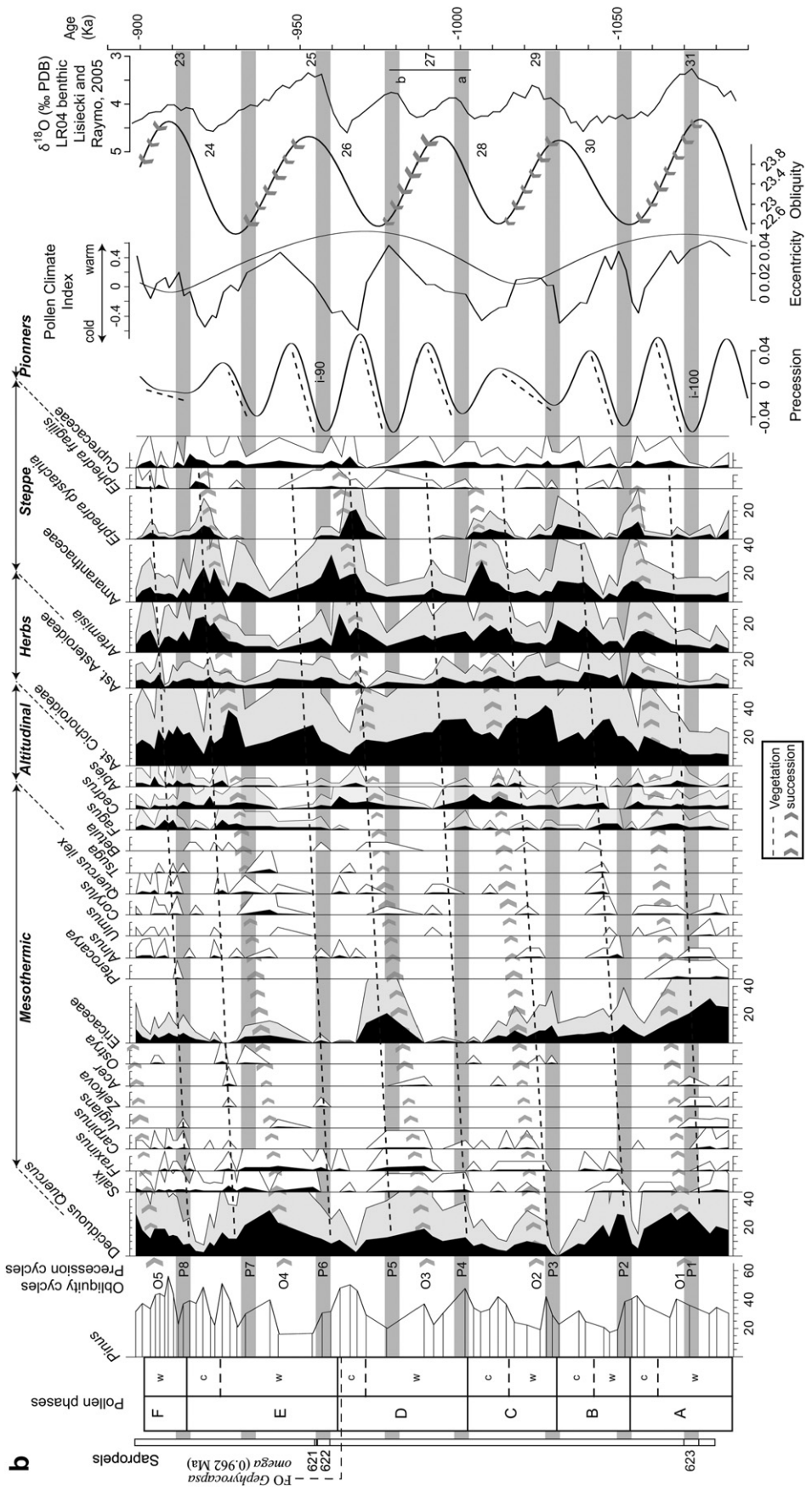

Fig. 7. (*continued*).

linked to the high percentages of Ericaceous pollen that today indicate wet and cool conditions (Ojeda et al., 1998) and clearly underestimate the "thermal optimums" evidenced during the interglacials both by the PCI and the winter precipitation curves. Only the temperature of the coldest month gives expected values for this period.

Quantitative climate reconstructions based on the ODP Site 976 pollen assemblages seem coherent. Excluding the Tertiary inherited taxa (*Liquidambar*, *Zelkova*, *Pterocarya* and *Tsuga*) of the MAT do not affect climate reconstructions in the present work. We unambiguously show that the MAT can successfully be applied to older periods, such as the MPT, when the presence of sub-tropical taxa is quasi-negligible.

5.3. Vegetation response to orbital forcing

5.3.1. Pollen-inferred vegetation dynamic

Based on our age-model, marine ($\delta^{18}O$, SST) and continental (pollen taxa, PCI) proxies from ODP Site 976 can be compared to the global benthic $\delta^{18}O$ record (LR04) and astronomical forcing functions (obliquity and precession index; Laskar et al., 2004) (Fig. 7a). Four complete and one incomplete vegetation successions (noted O1 to O5) broadly show a similar pattern characterized by the replacement of temperate trees (mainly *Quercus* deciduous and Ericaceae) by altitude elements (*Cedrus*, *Fagus*, *Abies*), and then by herbs and steppe maxima (Ast. Cichorioideae, Amaranthaceae, *Artemisia*, *Ephedra dystachia*). This similar, repetitive pattern eventually shows slight differences in taxa that constituted the ecosystems. Thus, Table 2 gives a detailed taxa list for each succession episode, including Cupressaceae (and sometimes *Pinus*) as the pioneers that probably initiated those vegetation successions. Asteraceae Cichorioideae shows a specific behavior as they developed during glacial–interglacial transitions (warmer and relatively dry climate) and interglacial-glacial transitions. Such vegetation changes are similar to those observed several times at Banyoles (Julià Bruguès and Suc, 1980; Leroy, 1988, 1997) and in other south-western Mediterranean sites during the whole Pleistocene (Combourieu Nebout et al., 1999, 2002; Sánchez-Goñi et al., 2002).

These taxa replacements clearly suggest the vegetation adaptation to climatic changes that evolved from warm-humid conditions towards arid-cold ones, with intermediate cooler but still humid climate, favourable to mountainous taxa development at time of transitions (e.g. Joannin et al., 2007a). Each of the five vegetation successions (O1–O5) started at an obliquity maximum. Those vegetation successions ended during glacials (heavy $\delta^{18}O$ intervals). Glacial–interglacial alternations are driven by obliquity changes during the first part of the MPT (Maslin and Ridgwell, 2005), and it is admitted that they responded linearly to insolation changes (Imbrie et al., 1993). Although our time series is too short for a meaningful test, we propose that PCI variations are also linearly related to obliquity forcing. They are not synchronous, however. Within the limits of our orbital tuning, it is important to notice, for instance, that MIS 30 (Bc), 28 (Cc), 26 (Dc) and 24 (Ec) lag the corresponding obliquity minima by some millennia.

One vegetation succession, in particular, drew our attention. It occurs between O1 and O2 and starts within pollen phase Bw (Fig. 7b). Successive large taxa dominances result in as high abundance values as those of O1 to O5 vegetation successions. Such an oscillation, which is internal to MIS 30, cannot be explained by the rather long-term obliquity forcing and requires an additional shorter time-scale forcing. Sapropel stratigraphy clearly indicates a marked regional climate response to precessional forcing. Such a vegetation succession, out of phase with the obliquity cycle, leads us to closely look the pollen diagram and to observe several successive arrangement of taxa development. As some of these successions are nearly in phase with succession related to obliquity cycles (maxima to minima), one must question whether they may be considered as independent successions resulting from superimposed orbital forcing or as subdued oscillations due to the combination of vegetation responses to obliquity and precession. Arguing that when they were out of phase, orbital parameters clearly induced decoupled vegetation responses, we choose to follow the first interpretation. Thus, eight short-lived

Table 2
Detailed taxa listed for each vegetation succession: the five, long-lasting, obliquity-related vegetation successions (O1–O5), and the eight short-lasting, precession-related vegetation successions (P1–P8) are organized in the same pattern.

Obliquity cycles	Warm	Transition	Cold	Pioneer
O5	D. *Quercus*, Ericaceae	–	–	–
O4	D. *Quercus*, *Frax.*, *Juglans*, Ericaceae, *Corylus*	*Fagus*, *Abies*	Ast. cicho. and ast., *Artemisia*, Amarant., *Ephedra dystachia* and *fragilis*	Cupressaceae, *Pinus*
O3	D. *Quercus*, *Frax.*, *Carpinus*, *Acer*, Ericaceae, *Corylus*	*Cedrus*	Ast. cicho., *Artemisia*, Amarant., *Ephedra dystachia*	Cupressaceae, *Pinus*
O2	D. *Quercus*, *Salix*, *Fraxinus*, Ericaceae, *Alnus*, *Corylus*	*Fagus*, *Cedrus*, *Abies*	Ast. ast., *Artemisia*, Amarant., *Ephedra dystachia*	Cupressaceae
O1	D. *Quercus*, *Salix*, Ericaceae, *Pterocarya*, *Alnus*, *Corylus*	*Fagus*, *Cedrus*	Ast. cicho. and ast., *Artemisia*, Amarant., *Ephedra dystachia*	Cupressaceae, *Pinus*
P8	D. *Quercus*, *Salix*, *Frax.*, *Juglans*, Ericaceae, *Pterocarya*	*Fagus*, *Abies*, *Pinus*	Ast. ast., *Artemisia*, Amarant., *Ephedra dystachia*	Cupressaceae
P7	D. *Quercus*, *Salix*, *Frax.*, *Zelkova*, *Acer*, Ericaceae, *Pterocarya*	*Fagus*, *Cedrus*, *Abies*, *Pinus*	Ast. cicho. and ast., *Artemisia*, Amarant., *Ephedra dystachia*	Cupressaceae, *Pinus*
P6 (sapropel 622 = *i*-90)	D. *Quercus*, *Frax.*, *Zelkova*, Ericaceae, *Alnus*	*Fagus*	Ast. cicho.	Cupressaceae
P5	D. *Quercus*, *Frax.*, Ericaceae	*Cedrus*, *Abies*	Ast. ast., *Artemisia*, Amarant., *Ephedra dystachia*	Cupressaceae, *Pinus*
P4	D. *Quercus*, *Salix*, Ericaceae, *Quercus ilex*	*Fagus*	Ast. cicho. and ast., *Artemisia*, Amarant.	Cupressaceae
P3	D. *Quercus*, *Frax.*, Ericaceae, *Alnus*, *Corylus*	*Fagus*, *Cedrus*, *Abies*	Ast. cicho., *Artemisia*, Amarant., *Ephedra dystachia*	Cupressaceae
P2	D. *Quercus*, *Salix*, *Frax.*, Ericaceae, *Alnus*, *Corylus*, *Q. ilex*	*Tsuga*, *Fagus*, *Cedrus*	Ast. cicho. and ast., *Artemisia*, Amarant., *Ephedra dystachia*	Cupressaceae
P1 (sapropel 623 = *i*-100)	D. *Quercus*, *Salix*, *Frax.*, *Carpinus*, *Juglans*, *Zelkova*, Ericaceae, *Pterocarya*, *Alnus*, *Corylus*	*Fagus*, *Cedrus*, *Abies*	*Ephedra dystachia*	Cupressaceae

vegetation successions are indicated (noted P1–P8; Fig. 7b). They show a similar repetitive pattern as the one previously described (temperature trees => altitude elements => steppe and herbs), broadly implying the same taxa (Table 2). P1, P2, P3, P4, P7 and P8 are the most easily identifiable successions. P5 and P7 are less clearly expressed as [1] they both took place in the interval over which the temporal resolution of our dataset is poor, and [2] P5 is nearly concomitant to O3 that probably masks it. P6 initiated contemporaneously to sapropel layer 622, and corresponds to a clearly recorded mesothermic phase (Table 2). Cold and arid phase of P6 succession is likely missed due to the low-temporal resolution, its ending takes place during the Cupressaceae rising. The mean duration of precession-related vegetation successions is ~23 kyr.

On the whole, the five, long-lasting, obliquity-related vegetation successions O1–O5, and the eight short-lasting, precession-related vegetation successions P1–P8 are organized with the same pattern and can only be discriminated by their duration. The sapropel deposits that correlate with precession minima strengthen our interpretation of a precession influence on the short-lasting vegetation changes P1–P8.

5.3.2. *Pollen-inferred vegetation response to orbital forcing*

The link between vegetation successions and climate cycles has been previously described for the last 800 kyr (e.g. Cheddadi et al., 2005; Tzedakis, 2007). The question remains largely unsolved for vegetation response to climate cycles driven by obliquity during the Early Pleistocene. Only a few studies from the Mediterranean area are sufficiently well dated to bring a clear insight on this puzzling question. Combourieu Nebout (1993) observed a vegetation succession scheme for the Pliocene vegetation, which was, however, too far in ecological terms to be compared with that from ODP Site 976. Ravazzi and Rossignol-Strick (1995) and Muttoni et al. (2007) observed an obliquity-related climatic cycle resulting in vegetation successions in the Leffe Basin (Italy). However the MIS stratigraphy (and, thus, the orbital chronology) is not certain, which makes it difficult to clearly address the problem of vegetation response to astronomical forcing. In the Santa Lucia section (1.36–1.28 Ma), Joannin et al. (2007a) observed two obliquity-related vegetation successions and climatic cycles (MIS 43–40), while three vegetation successions also revealed the superimposed precession influence. In fact, two precession-related vegetation successions were, actually concomitantly driven by obliquity forcing. The ODP Site 976 pollen record extends, therefore, the observed obliquity-related vegetation successions over the first half of the MPT. Because of its impacts on insolation at high northern latitudes, obliquity drives ice volume and high-latitude temperature changes recorded in the benthic $\delta^{18}O$ over the MPT (Maslin and Ridgwell, 2005). Obliquity has less effect than precession on insolation at low latitudes such as in southern Spain. Thus, it is likely that, during the first half of the MPT, the climate system and, therefore, the vegetation in the Mediterranean area mainly responded to obliquity forcing through remote impacts of global climate changes driven at higher latitudes.

As for the Santa Lucia Section (Joannin et al., 2007a), we observed precession-related vegetation successions in addition to obliquity-related ones in ODP Site 976. This implies that climate and vegetation responded to both orbital parameters during the first half of the MPT. Precessional forest vegetation cycles within longer-term, obliquity-dominated glacial/interglacial cycles are also suspected in the pollen record from Leffe basin (Italy; Tzedakis, 2007). According to this author the total AP curve could suggest a 30 kyr-long interglacial, while a closer inspection shows distinct forest vegetation successions that responded to precessional insolation cycles. Our observation leads to the same conclusion in the lowermost part of the ODP Site 976 record. There, the onset of vegetation succession P2 clearly drove the PCI to higher values than those expected during this glacial phase MIS 30 (Fig. 7b). In a classical pollen interpretation, pollen phases Aw-c and Bw would have been both associated with MIS 31. In Tenaghi Philippon pollen record, the AP curve shows a continuous warm pollen phase (lasting 50 kyr, from 1.09 to 1.04 Ma) attributed to MIS 31 (Tzedakis, 2007, Fig. 8). The *Quercus* percentage curve clearly illustrates a first warm steady pollen phase related to MIS 31 (lasting 20 kyr, from 1.09 to 1.07 Ma) and second one (lasting 20 kyr, from 1.06 to 1.04 Ma) which is contemporaneous to Bw (1.055–1.04 Ma) and appears, therefore, to be forced by precession. Our observation also implies that, during the first half of the MPT, vegetation successions driven by precession forcing are not less complete or less dramatic than vegetation changes driven by obliquity. As for obliquity-forced vegetation successions, the precession-driven, vegetation changes correspond to temperate trees being replaced by altitudinal elements and, then, steppe herbs, as if the climate deterioration was of similar amplitude in both cases.

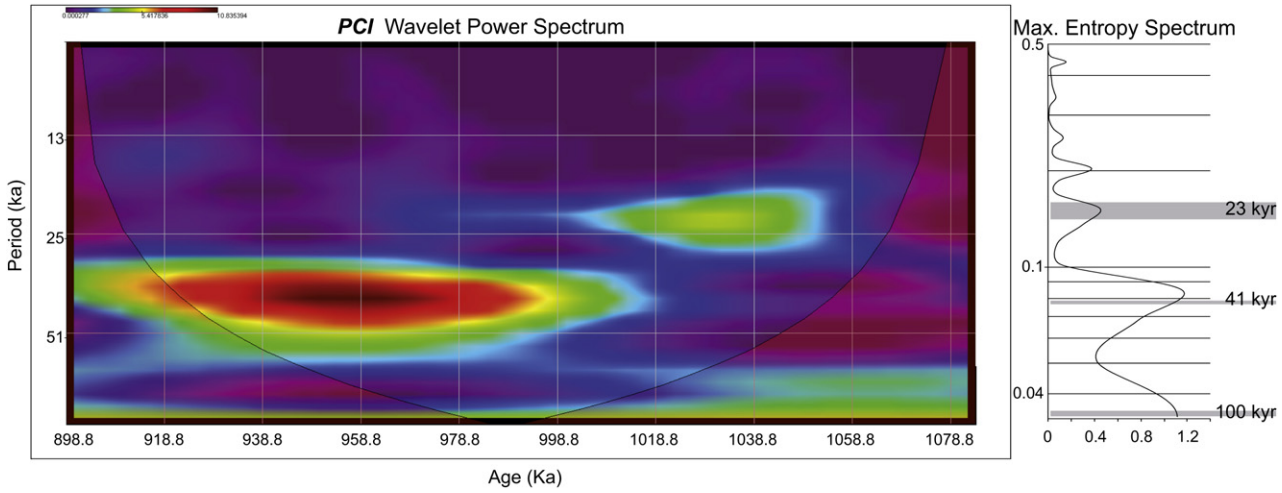

Fig. 8. Spectral and Wavelet analysis of pollen climate index (PCI). PCI values have been re-sampled using a simple, cubic spline function (*Analyseries* software, version 1.05; Paillard et al., 1996). Then MEM analyses were carried out with the *Strati-Signal* software (version 1.0.5, University of Geneva; Ndiaye, 2007). The colouring scale is on a logarithmic arbitrary amplitude scale where purple and red characterized weak and strong power, respectively. Western Mediterranean experienced a shift at 1.01 Ma from precession frequencies (1.05–1.01 Ma) to strong obliquity frequencies (1.01–0.9 Ma) (For interpretation of the reference to colour in this figure legend, the reader is referred to the web version of this article).

Fig. 7b shows that PCI maxima precisely follow the eccentricity curve. Low-latitude insolation is mainly forced by precession, which is modulated in terms of amplitude by eccentricity (Lisiecki, 2010). It is expected, therefore, that climate and vegetation changes in the Mediterranean area can reveal to some extent the eccentricity signal and, more particularly the ~100 kyr oscillation. However, obliquity forcing is independent from eccentricity, and it is odd to observe the apparent 100 kyr modulation of the long-term (obliquity-related), PCI cycles. It is likely that this apparent modulation is ultimately associated to the combination of short (precession-related) and long (obliquity-related) vegetation cycles. In other words, although obliquity-related oscillations clearly dominate the PCI record, the amplitude of these oscillations may result to a large extent from the presence of "internal", shorter precession oscillations (which would be modulated by eccentricity). These precession-related oscillations do not show up clearly in the PCI records, but they are obviously present in the pollen records, where they are associated to the P1–P8 vegetation changes. Joannin et al. (2007a) made a preliminary observation of a vegetation change linked to the eccentricity in the Santa Lucia deposits (Italy). In both his and our study, records are too short to confidently test and explain the ~100 kyr modulation. Additional, longer records are needed to correctly address this question.

5.3.3. Spectral analysis of the PCI record

The maximum entropy spectral analysis indicates that obliquity-related oscillation (41 kyr) is the dominant oscillation embedded in our PCI record (Fig. 8). Such an observation is in good accordance with the well-known dominance of the obliquity forcing during the first half of the MPT, and with a previous work on the vegetation response to obliquity (Tzedakis et al., 2006). Wavelet analysis makes it possible to look at potential spectral evolution within the PCI series. As expected from the MEM results, a strong response is observed at the obliquity period (41 kyr), but only from 1.01 to 0.9 Ma. The precession period, on the other hand, is only clearly recorded from 1.05 to 1.01 Ma. The 100 kyr component cannot be discussed confidently as the record only covers 190 kyr, and, as suggested by several works, the 100 kyr oscillation progressively develops around MPT but became a dominant feature of the global climate much later, around 600 kyr.

Spectral analysis on AP data helps to interpret vegetation and climate response to orbital parameters. On the well-known Tenaghi Philippon Sequence, Tzedakis et al. (2006) found strong responses to eccentricity, obliquity and precession forcings. In details and in the state of the current knowledge, they did not observe strong precession frequencies between 1.3 and 0.85 Ma. These observations, plus an SST wavelet analysis (Lourens et al., 1992), lead them to conclude that "taken together, these results underscore the pervasive influence of precession on Mediterranean climates, including the interval of the 41 kyr world". Based on the vegetation dynamic analysis, ODP Site 976 vegetation successions reveal two overlapping rhythms related to vegetation and climate responses to obliquity and precession parameters during the whole studied interval (1.09–0.9 Ma). However, our wavelet analyses of PCI parameter show that obliquity and precession were not recorded, together, continuously over the studied interval. These wavelet analyses suggest that vegetation (and climate) in the Western Mediterranean experienced a shift at 1.01 Ma from precession frequencies (1.05–1.01 Ma) to strong obliquity frequencies (1.01–0.9 Ma). Yet, as we have seen above, precession-related changes are clearly embedded in the pollen records across the whole studied interval (i.e. the P1–P8 vegetation changes). Such an apparent discrepancy between vegetation dynamic analysis and wavelet analysis of the PCI record could be due to the fact that the principal component analysis does not successfully catch the full complexity of superimposed vegetation dynamics and is not able, therefore, to pass on short-time climate dynamics like precession cycles in the presence of stronger amplitude obliquity cycles.

One important conclusion of our work is that PCI or AP curves are useful to study climate changes. However, used alone, such records can be misleading and let the palynologists miss the complex signal resulting from the internal vegetation dynamic and its response to orbital forcing.

5.3.4. MPT potential

Compared with the entire Pleistocene, the MPT can be considered as an abrupt climate change (Rial, 2004) that leads some author to re-name the MPT as MPR "Mid-Pleistocene Revolution" (e.g. Berger and Jansen, 1994; Bassinot et al., 1997; Maslin and Ridgwell, 2005). On the other hand, the ice-sheet glacial occurrences during the MPT are also expected to characterize more intense and prolonged glacial states with associated subsequent rapid deglaciations (Maslin and Ridgwell, 2005).

Precession-related climatic oscillations, typical of low latitudes, are recorded in marine sedimentary records from the Mediterranean basin since the Pliocene (Kroon et al., 1998). We expected that this precession signature would be enhanced in our pollen records at the MPT, since the progressive onset of the "100 kyr world is clearly associated with a relative decrease of the obliquity response in the global climate. But obliquity and precession-related changes are both observed across the entire studied interval in our pollen records. And the PCI record shows a result opposite to what is expected, with the dominance of the obliquity signal in the upper part of the studied interval. Thus, as for the Central Mediterranean (Joannin et al., 2007a, 2008), the pollen-inferred Early Pleistocene vegetation dynamic (and climate) of the Western Mediterranean region does not clearly evidence a decrease of the obliquity response relative to the precession signal at the onset of the MPT. One possibility to explain this observation is that this change in dominance occurred during the second half of the MPT (i.e. 0.900–0.600 Ma), beyond the scope of the present study.

Marine sediments from the Mediterranean Sea provide among the best records spanning the Late/Early Pleistocene and MPT, making it possible to better constrain vegetation, climate, and carbon-cycle responses to orbital forcing (with a focus on the 41 kyr world) as asked by Lisiecki (2010). Tzedakis et al. (2009) evidenced, on orbital and millennial time scales, relationships between atmospheric greenhouse gas concentrations and vegetation variations for the eight last climate cycles. Such studies really need to be extended further in the past with independent chronological tools.

6. Conclusion

At ODP Site 976, Pleistocene deep-sea sediments are a combination of repetitive turbidite mud layers, which suggest a southern Iberia margin source, embedded in hemipelagic sediments. Clays and palynomorphs indicate both river- and wind-transported pollen grains. The pollen record, therefore, documents vegetation and climatic changes in the Western Mediterranean.

To resolve discrepancies between the original $\delta^{18}O$-derived and SST-derived stratigraphies at the beginning of the MPT, we had [1] to compare the pollen-inferred first Factor pollen climate index (PCI) with a regional oxygen isotope record from the Ionian Sea (KC01b) and with the global, LR04 benthic oxygen isotope stack, and [2] to downward extend the studied interval and add up-to-date bio-events information. We put forward a revised age calibration that ran from MIS 31 (~1.09 Ma at ~260 mcd) to MIS 23 (~0.90 Ma at ~230 mcd) and, therefore, propose a revised age-model for the studied interval. It gives an estimate for the average sedimentation accumulation rate of 0.157 m/kyr.

From the pollen record, the absence of sub-tropical taxa, such as *Cathaya*, Taxodiaceae and *Carya*, supplies information on the late Early Pleistocene climatic conditions that experienced reduced

temperature and wetness. In this context, the interglacial MIS 31 appears to be an exceptional long period, with particularly warm conditions in the Mediterranean area. *Pterocarya* and *Zelkova* pollen rarefy in the following interglacials, which probably announces their close extinction in Southern Iberia. Quantitative climate reconstructions show unambiguously that the modern analogues technique (MAT) can successfully be applied to older periods, such as the MPT, when the presence of sub-tropical taxa is quasi-negligible. Reconstructions mimic glacial–interglacial phases recorded by the PCI. The observed winter temperature anomalies of about −5 °C for older cold phases are in the range of glacial temperature reconstructions for the Early Pleistocene in the Mediterranean area, whereas the reconstructed −10 °C cooling for the following cold phases seem methodologically biased due to the lack of modern analogues.

Further back in time, we evidenced climatically-induced vegetation changes, which are characterized by the replacement of temperate trees and shrubs, such as oak and heath, by mountain taxa, and then by herbs and steppe taxa (Ast. Cichorioideae, Amaranthaceae, Artemisia, Ephedra dystachia). Pioneers heliophylous Cupressaceae (and sometimes *Pinus*) initiated vegetation successions. Over the studied interval, five long-lasting, obliquity-related vegetation successions O1–O5, and eight short-lasting, precession-related vegetation successions P1–P8 are organized with the same pattern and can only be discriminated by their duration. Only the forest phase of the precession-related vegetation succession is usually described in the Mediterranean. Our observations imply, therefore, that the vegetation succession that takes place during a half precession cycle is not limited to a change of forest trees, but corresponds to a drastic vegetation change, including a final steppe phase under deteriorated climate conditions.

Spectral and wavelet analysis on AP or PCI data helps to interpret vegetation and climate response to orbital parameters. While, for the Tenaghi Philippon Sequence in the eastern Mediterranean, Tzedakis et al. (2006) did not observe strong precession frequencies between 1.3 and 0.85 Ma, our data from the western Mediterranean indicate a shift at 1.01 Ma from precession frequencies (1.05–1.01 Ma) to strong obliquity frequencies (1.01–0.9 Ma). The apparent discrepancy between our vegetation dynamic analysis and wavelet analysis of the PCI record could be due to the fact that the principal component analysis does not successfully catch the full complexity of superimposed vegetation dynamics and is, therefore, less likely to show short-time climate dynamics like precession cycles in the presence of stronger amplitude obliquity cycles. PCI or AP curves appear useful to study climate changes and may be considered equivalent climate proxy to isotope one. However, used alone, such records can be misleading and let the palynologists miss the complex signal resulting from the internal vegetation dynamic and its response to orbital forcing.

As for the Central Mediterranean (Joannin et al., 2007a, 2008), the pollen-inferred Early Pleistocene vegetation dynamic (and climate) of the Western Mediterranean region does not show a decrease of the obliquity response relative to the precession response at the onset of the MPT.

Acknowledgment

We thank P.C. Tzedakis and one anonymous reviewer for discussion and appreciable improvements of this manuscript. This study used samples provided by the Ocean Drilling Program, which is sponsored by the US National Science Foundation and participating countries under the management of the Joint Oceanographic Institutions, Inc. This work is part of a Ph.D. thesis financed by the French Ministry for Research and Technology. The authors are grateful to CNRS and to UMR 5125 for financial support. We particularly thank Jean-Pierre Suc who supervised this thesis and Lysiane Thévenod for technical support. The authors are grateful to José M. González-Donoso for providing SST record.

Appendix A. Supplementary data

Supplementary data related to this article can be found online at doi:10.1016/j.quascirev.2010.11.009.

References

Agustí, J., Blain, H.A., Furió, M., De Marfá, R., Santos-Cubedo, A., 2010. The early Pleistocene small vertebrate succession from the Orce region (Guadix-Baza Basin, SE Spain) and its bearing on the first human occupation of Europe. Quaternary International 223, 162–169.

Aloisi, J.-C., 1986. Sur un modèle de sédimentation deltaïque. Contribution à laconnaissance des marges passives. University Perpignan, France, PhD thesis.

Alonso, B., Ercilla, G., Martínez-Ruíz, F., Baraza, J., Galimony, A., et al., 1999. Pliocene-Pleistocene sedimentary facies at site 976: depositional history in the northwestern Alboran sea. In: Zahn, R., Comas, M.C., Klaus, A., et al. (Eds.). Proceeding of the Ocean Drilling Program, Scientific Results, College Station. TX, pp. 57–68. vol. 161, Ocean Drilling Program.

Bassinot, F.C., Beaufort, L., Vincent, E., Labeyrie, L., 1997. Changes in the Dynamics of Western Equatorial Atlantic Surface Currents and Biogenic Productivity at the "Mid-Pleistocene Revolution" (~930 ka), vol. 154. Proceedings of the Ocean Drilling Program. Scientific, Scientific Results, pp. 269–284.

Beaudouin, C., Dennielou, B., Melki, T., Guichard, F., Kallel, N., Berné, S., Huchon, A., 2004. The Late-Quaternary climatic signal recorded in a deep-sea turbiditic levee (Rhône Neofan, Gulf of Lions, NW Mediterranean): palynological constraints. Sedimentary Geology 172, 85–97.

Beaudouin, C., Suc, J.-P., Cambon, G., Touzani, A., Giresse, P., Pont, D., Aloïsi, J.C., Marsset, T., Cochonat, P., Duzer, D., Ferrier, J., 2005. Present-day rhythmic deposition in the Grand Rhone prodelta (NW Mediterranean) according to high-resolution pollen analyses. Journal of Coastal Research 21, 292–306.

Beaudouin, C., Suc, J.-P., Escarguel, G., Arnaud, M., Charmasson, S., 2007. The significance of pollen record from marine terrigenous sediments: the present-day example of the Gulf of Lions (Northwestern Mediterranean Sea). Geobios 40, 159–172.

Berger, W.H., Jansen, E., 1994. Mid-Pleistocene climate shift: the Nansen connection. In: Johannessen, O.M., Muench, R.D., Overland, J.E. (Eds.), The Polar Oceans and Their Role in Shaping the Global Environment, vol. 85, pp. 295–311. Geophysical Monograph.

Berger, A., Loutre, M.F., 2004. Théorie astronomique des paléoclimats. Comptes Rendus Géoscience 336, 701–709.

Bernasconi, S.M., Meyers, P.A., O'Sullivan, G., 1999. Early diagenesis in rapidly accumulating sediments on the Alboran slope, ODP site 976. Geo-Marine Letters 18, 209–214.

Bertini, A., Ciaranfi, N., Marino, M., Palombo, M.R., 2010. Proposal for Pliocene and Pleistocene land–sea correlation in the Italian area. Quaternary International 209, 95–108.

Birks, H.J.B., Birks, H.H., 2004. The rise and fall of forests. Science 305, 484–485.

Bonnefille, R., Potts, R., Chalié, F., Jolly, D., Peyron, O., 2004. High-resolution vegetation and climate change associated with Pliocene Australopithecus afarensis. Proceedings of the National Academy of Sciences 101, 12125–12129.

Bout-Roumazeilles, V., Combourieu Nebout, N., Peyron, O., Cortijo, E., Landais, A., Masson-Delmotte, V., 2007. Connection between South Mediterranean climate and North African atmospheric circulation during the last 50,000 yr BP North Atlantic cold events. Quaternary Science Reviews 26, 3197–3215.

Brewer, S., Guiot, J., Sánchez-Goñi, M.F., Klotz, S., 2008. The climate in Europe during the Eemian: a multi-method approach using pollen data. Quaternary Science Reviews 27, 2303–2315.

Cambon, G., Suc, J.-P., Aloisi, J.-C., Giresse, P., Monaco, A., Touzani, A., Duzer, D., Ferrier, J., 1997. Modern pollen deposition in the Rhône delta area (lagoonal and marine sediments), France. Grana 36, 105–113.

Capraro, L., Asioli, A., Backman, J., Bertoldi, R., Channell, J.E.T., Massari, F., Rio, D., 2005. Climatic patterns revealed by pollen and oxygen isotope records across the Brunhes-Matuyama boundary in the Central Mediterranean (Southern Italy). In: Head, M.J., Gibbard, P.L. (Eds.), Early–Middle Pleistocene Transitions: The Land–Ocean Evidence. Geological Society London, Spec. Publ., vol. 247, pp. 159–182.

Cheddadi, R., Lamb, H.F., Guiot, J., van der Kaars, S., 1998. Holocene climatic change in Morocco: a quantitative reconstruction from pollen data. Climate Dynamics 14, 883–890.

Cheddadi, R., de Beaulieu, J.L., Jouzel, J., Andrieu-Ponel, V., Laurent, J.M., Reille, M., Raynaud, D., Bar-Hen, A., 2005. Similarity of vegetation dynamics during interglacial periods. Proceedings of the National Academy of Sciences 102, 13939–13943.

Combourieu Nebout, N., 1987. Les premiers cycles glaciaire-interglaciaire en région méditerranéenne d'après l'analyse palynologique de la série plio-pléistocène de Crotone (Italie méridionale). University Montpellier 2, France, PhD thesis.

Combourieu Nebout, N., 1993. Vegetation response to Upper Pliocene glacial/interglacial cyclicity in the Central Mediterranean. Quaternary Research 40, 228–236.

Combourieu Nebout, N., Vergnaud Grazzini, C., 1991. Late Pliocene northern hemisphere glaciations: the continental and marine responses in the central Mediterranean. Quaternary Science Reviews 10, 319–334.
Combourieu Nebout, N., Londeix, L., Baudin, F., Turon, J.L., von Grafenstein, R., Zahn, R., et al., 1999. Quaternary marine and continental paleoenvironments in the western mediterranean (site 976, Alboran Sea): palynological evidence. In: Zahn, R., Comas, M.C., Klaus, A., et al. (Eds.). Proceeding of the Ocean Drilling Program, Scientific Results, College Station. TX, pp. 457–468. vol. 161, Ocean Drilling Program.
Combourieu Nebout, N., Turon, J.L., Zahn, R., Capotondi, L., Londeix, L., Pahnke, K., 2002. Enhanced aridity and atmospheric high-pressure stability over the western Mediterranean during the North Atlantic cold events of the past 50 k.y. Geology 30, 863–866.
Combourieu Nebout, N., Peyron, O., Dormoy, I., Desprat, S., Beaudouin, C., Kotthoff, U., Marret, F., 2009. Climatic variability in the west Mediterranean during the last 25,000 years from pollen data. Climate of the Past 5, 503–521.
Cour, P., 1974. Nouvelles techniques de détection des flux et de retombées polliniques: étude de la sédimentation des pollens et des spores à la surface du sol. Pollen et Spores 16, 103–141.
Davis, B., Brewer, S., 2009. Orbital forcing and role of the latitudinal insolation/temperature gradient. Climate Dynamics 32, 143–165.
Davis, B.A.S., Brewer, S., Stevenson, A.C., Guiot, J., 2003. The temperature of Europe during the Holocene reconstructed from pollen data. Quaternary Science Reviews 22, 1701–1716.
De Beaulieu, J.L., Andrieu-Ponel, V., Cheddadi, R., Guiter, F., Ravazzi, C., Reille, M., Rossi, S., 2006. Apport des longues séquences lacustres à la connaissance des variations des climats et des paysages pléistocènes. C.R. Paleo 5, 65–72.
De Kaenel, E., Siesser, W.G., Murat, A., 1999. Pleistocene calcareous nannofossil biostratigraphy and the western Mediterranean sapropels, Site 974 to 977 and 979. In: Zahn, R., Comas, M.C., Klaus, A., et al. (Eds.). Proceeding of the Ocean Drilling Program, Scientific Results, College Station. TX, pp. 159–183. vol. 161, Ocean Drilling Program.
De Vernal, A., 2009. Marine palynology and its use for studying nearshore environments. In: From Deep-sea to Coastal Zones: Methods and Techniques for Studying Paleoenvironments, vol. 5. IOP Conf. Series:Earth and Environmental Science, pp. 1–12. doi:10.1088/1755-1307/5/1/012002.
Diniz, F., 1984. Apports de la palynologie à la connaissance du Pliocène portugais. Rio Maior: un bassin de référence pour l'histoire de la flore, de la végétation et du climat de la façade atlantique de l'Europe méridionale. University Montpellier 2, France, PhD thesis.
Dormoy, I., Peyron, O., Combourieu Nebout, N., Goring, S., Kotthoff, U., Magny, M., Pross, J., 2009. Terrestrial climate variability and seasonality changes in the Mediterranean region between 15,000 and 4,000 years BP deduced from marine pollen records. Climate of the Past 5, 615–632.
Emeis, K.-C., Shulz, H., Struck, U., Rossignol-Strick, M., Erlenkeuser, H., Howell, M.W., Kroon, D., Mackensen, A., Ishizuka, S., Oba, T., Sakamoto, T., Koizumi, I., 2003. Eastern Mediterranean surface water temperatures and d1k8O composition during deposition of sapropels in the late Quaternary. Paleoceanography 18, 1–18.
Fabrés, J., Calafat, A., Sánchez-Vidal, A., Canals, M., Heussner, S., 2002. Composition and spatio-temporal variabilityof particle fluxesin the Western Alboran Gyre, Mediterranean Sea. Journal of Marine Systems 33, 431–456.
Fauquette, S., Guiot, J., Suc, J.-P., 1998. A method for climatic reconstruction of the Mediterranean Pliocene using pollen data. Palaeogeography, Palaeoclimatology, Palaeoecology 144, 183–201.
Fletcher, W.J., Sánchez-Goñi, M.F., 2008. Orbital- and sub-orbital-scale climate impacts on vegetation of the western Mediterranean basin over the last 48,000 yr. Quaternary Research 70, 451–464.
Fletcher, W.J., Sánchez-Goñi, M.F., Peyron, O., Dormoy, I., 2010. Abrupt climate changes of the last deglaciation detected in a western Mediterranean forest record. Climate of the Past 6, 245–264.
Follieri, M., 2010. Conifer extinction in Quaternary Italian records. Quaternary International 225, 37–43.
Fusco, F., 2010. Picea ± *Tsuga* pollen record as a mirror of oxygen isotope signal? An insight into the Italian long pollen series from Pliocene to Early Pleistocene. Quaternary International 225, 58–74.
González-Donoso, J.M., Serrano, F., Linares, D., 2000. Sea surface temperature during the Quaternary at ODP Sites 976 and 975 (western Mediterranean). Palaeogeography, Palaeoclimatology, Palaeoecology 162, 17–44.
Guiot, J., 1990. Methodology of the last climatic cycle reconstruction in France from pollen data. Palaeogeography, Palaeoclimatology, Palaeoecology 80, 49–69.
Hammer, ø, Harper, D.A.T., Ryan, P.D., 2001. PAST: paleontological statistics software package for education and data analysis. Palaeontologia Electronica 4, pp. 9.
Head, M.J., Gibbard, P.L., 2005. Early–Middle Pleistocene transitions: an overview and recommendation for the defining boundary. In: Head, M.J., Gibbard, P.L. (Eds.), Early–Middle Pleistocene Transitions: The Land-Ocean Evidence, Geological Society. London, Spec. Publ., vol. 247, pp. 1–18.
Heusser, L.E., 1988. Pollen distribution in marine sediments on the continental margin off northern California. Marine Geology 80, 131–147.
Hooghiemstra, H., Lézine, A.M., Leroy, S.A.G., Dupont, L., Marret, F., 2006. Late Quaternary palynology in marine sediments: a synthesis of the understanding of pollen distribution patterns in the NW African setting. Quaternary International 148, 29–44.
Hutson, W., 1980. The Agulhas current during the Late Pleistocene: analysis of modern faunal analogs. Science 207, 64–66.
Imbrie, J., Berger, A., Boyle, E.A., Clemens, S.C., Duffy, A., Howard, W.R., Kukla, G., Kutzbach, J., Martinson, D.G., McIntyre, A., Mix, A.C., Molfino, B., Morley, J.J., Peterson, L.C., Pisias, N.G., Prell, W.L., Raymo, M.E., Shackleton, N.J., Toggweiler, J.R., 1993. On the structure and origin of major glaciations cycles 2. The 100,000-year cycle. Paleoceanography 8, 699–735.
Jiménez-Moreno, G., Fauquette, S., Suc, J.-P., 2010. Miocene to Pliocene vegetation reconstruction and climate estimates in the Iberian Peninsula from pollen data. Review of Palaeobotany and Palynology 162, 403–415. doi:10.1016/j.revpalbo.2009.08.001.
Joannin, S., 2007. Changements climatiques en Méditerranée à la transition Pléistocène inférieur-moyen: pollens, isotopes stables et cyclostratigraphie. University Lyon 1, France, PhD thesis.
Joannin, S., Quillévéré, F., Suc, J.-P., Lécuyer, C., Martineau, F., 2007a. Early Pleistocene climate changes in the central Mediterranean region as inferred from integrated pollen and planktonic foraminiferal stable isotope analyses. Quaternary Research 67, 264–274.
Joannin, S., Cornée, J.J., Moissette, P., Suc, J.-P., Koskeridou, E., Lécuyer, C., Buisine, C., Kouli, K., Ferry, S., 2007b. Changes in vegetation and marine environments in the eastern mediterranean (Rhodes Island, Greece) during the early and middle Pleistocene. Journal of Geological Society of London 164, 1119–1131.
Joannin, S., Ciaranfi, N., Stefanelli, S., 2008. Vegetation changes during the late early Pleistocene at Montalbano Jonico (Province of Matera, southern Italy) based on pollen analysis. Palaeogeography, Palaeoclimatology, Palaeoecology 270, 92–101.
Joannin, S., Cornée, J.J., Münch, P., Fornari, M., Vasiliev, J., Krijgsman, W., Nahapetyan, S., Gabrielyan, Y., Ollivier, V., Roiron, P., Chataigner, C., 2010. Early Pleistocene climatic cycles in continental deposits of the Lesser Caucasus of Armenia inferred from palynology, magnetostratigraphy, and $^{40}Ar/^{39}Ar$ dating. Earth and Planetary Science Letters 291, 149–158.
Julià Bruguès, R., Suc, J.-P., 1980. Analyse pollinique des dépôts lacustres du Pléistocène inférieur de Banyoles (Bañolas, site de la Bòbila Ordis - Espagne): un élément nouveau dans la reconstitution de l'histoire paléoclimatique des régions méditerranéennes d'Europe occidentale. Geobios 3, 5–19.
Klotz, S., Fauquette, S., Combourieu Nebout, N., Uhl, D., Suc, J.P., Mosbrugger, V., 2006. Seasonality intensification and long-term winter cooling as a part of the Late Pliocene climate development. Earth and Planetary Science Letters 241, 174–187.
Kotthoff, U., Pross, J., Müller, U.C., Peyron, O., Schmiedl, G., Schulz, H., Bordon, A., 2008. Climate dynamics in the borderlands of the Aegean Sea during formation of Sapropel S1 deduced from a marine pollen record. Quaternary Science Reviews 27, 832–845.
Kroon, D., Alexander, I., Little, M., Lourens, L.J., Matthewson, A.H.F., Sakamoto, T., 1998. Oxygen isotope and sapropel stratigraphy in the Eastern Mediterranean during the last 3.2 million years. In: Roberton, A.H.F., Emeis, K.-C., Ritcher, C., et al. (Eds.). Proceedings of the Ocean Drilling Program, Scientific Results, College Station, TX, pp. 181–189. vol. 160, Ocean Drilling Program.
Laskar, J., Robutel, P., Joutel, F., Gastineau, M., Correia, A.C.M., Levrard, B., 2004. A long-term numerical solution for the insolation quantities of the Earth. Astronomy and Astrophysics 428, 261–285.
Leroy, S.A.G., 1988. Image pollinique d'une steppe du Pliocène supérieur à Bòbila Ordis, Banyoles (Catalogne), vol. XXV. Inst. Fr. Pondichéry, pp. 197–207.
Leroy, S.A.G., 1997. Climatic and non-climatic lake-level changes inferred from a Plio-Pleistocene lacustrine complex of Catalonia (Spain): palynology of the Tres Pins sequences. Journal of Paleolimnology 17, 347–367.
Lisiecki, L.E., 2010. Links between eccentricity forcing and the 100,000-year glacial cycle. Nature Geosciences 3, 349–352.
Lisiecki, L.E., Raymo, M.E., 2005. A Pliocene–Pleistocene stack of 57 globally distributed benthic $\delta^{18}O$ records. Paleoceanography 20, 1–17. doi:10.1029/2004PA001071.
Lisiecki, L.E., Raymo, M.E., 2007. Plio-Pleistocene climate evolution: trends and transitions in glacial cycle dynamics. Quaternary Science Reviews 26, 56–69.
Liu, Z., Herbert, T.D., 2004. High-latitude influence on the eastern equatorial Pacific climate in the early Pleistocene epoch. Nature 427, 720–723.
Lourens, L.J., 2004. Revised tuning of Ocean Drilling Program Site 964 and KC01B (Mediterranean) and implications for the delta O-18, tephra, calcareous nannofossil, and geomagnetic reversal chronologies of the past 1.1 Myr. Paleoceanography 19, PA3010. doi:10.1029/2003PA000997.
Lourens, L.J., Hilgen, F.J., Gudjonsson, L., Zachariasse, W.J., 1992. Late Pliocene to early Pleistocene astronomically forced sea surface productivity and temperature variations in the Mediterranean. Marine Micropaleontology 19, 49–78.
Lourens, L.J., Antonarakou, A., Hilgen, F.J., van Hoof, A.R.M., Vergnaud-Grazzini, C., Zachariasse, W.J., 1996. Evaluation of the Plio-Pleistocene astronomical timescale. Paleoceanography 11, 391–413.
Magri, D., 2010. Persistence of tree taxa in Europe and Quaternary climate changes. Quaternary International 219, 145–151.
Magri, D., Parra, I., 2002. Late Quaternary western Mediterranean pollen records and African winds. Earth and Planetary Science Letters 200, 401–408.
Magri, D., Di Rita, F., Palombo, M.R., 2010. An Early Pleistocene interglacial record from an intermontane basin of central Italy (Scoppito, L'Aquila). Quaternary International 225, 106–113.
Martínez-Ruíz, F., Comas, M.C., Alonso, B., 1999. Mineral associations and geochemical indicators in upper Miocene to Pleistocene sediments in the Alboran Basin. In: Zahn, R., Comas, M.C., Klaus, A., et al. (Eds.). Proceeding of the Ocean Drilling Program, Scientific Results, College Station. TX, pp. 21–36. vol. 161, Ocean Drilling Program.
Maslin, M.A., Ridgwell, A.J., 2005. Mid-Pleistocene Revolution and the 'eccentricity myth'. In: Head, M.J., Gibbard, P.L. (Eds.), Early–Middle Pleistocene Transitions: The Land–Ocean Evidence. Geological Society, London, Special Publications, vol. 247, pp. 19–34.

Mommersteeg, H.J.P.M., Loutre, M.F., Young, R., Wijmstra, T.A., Hooghiemstra, H., 1995. Orbital forced frequencies in the 975,000 year pollen record from Tenaghi Philippon (Greece). Climate Dynamics 11, 4–24.

Moscariello, A., Ravazzi, C., Brauer, A., Chiesa, S., Mangili, C., De Beaulieu, J.L., Reille, M., Rossi, S., 2000. A long lacustrine record from the Pianico-Sé Ilere-Sellere basin (Middle–Late Pleistocene, northern Italy). Quaternary International 73/74, 47–78. Special Issue 'Mediterranean Lacustrine Records'.

Mudelsee, M., Stattegger, K., 1997. Exploring the structure of the mid-Pleistocene revolution with advanced methods of time series analysis. Geologische Rundschau 86, 499–511.

Muttoni, G., Ravazzi, C., Breda, M., Pini, R., Laj, C., Kissel, C., Mazaud, A., Garzanti, E., 2007. Magnetostratigraphic dating of an intensification of glacial activity in the southern Italian Alps during Marine Isotope Stage 22. Quaternary Research 67, 161–173.

Naughton, F., Sanchez Goñi, M.F., Desprat, S., Turon, J.-L., Duprat, J., Malaizén, B., Joli, C., Cortijo, E., Drago, T., Freitas, M.C., 2007. Present-day and past (last 25000 years) marine pollen signal off western Iberia. Marine Micropaleontology 62 (2), 91–114.

Ndiaye, M., 2007. A multipurpose software for Stratigraphic Signal Analysis. University Geneva, Switzerland. http://archive-ouverte.unige.ch/vital/access/manager/Repository/unige: 717, PhD thesis.

Ojeda, F., Arroyo, J., Marañón, T., 1998. The phytogeography of European and Mediterranean heath species (Ericoideae, Ericaceae): a quantitative analysis. Journal of Biogeography 25, 165–178.

Okuda, M., Van Vugt, N., Nakagawa, T., Ikeya, M., Hayashida, A., Yasuda, Y., Setoguchi, T., 2002. Palynological evidence for the astronomical origin of lignite-detritus sequence in the Middle Pleistocene Marathousa Member, Megalopolis, SW Greece. Earth and Planetary Science Letters 201, 143–157.

Paillard, D., Labeyrie, L., Yiou, P., 1996. Macintosh program performs time-series analysis. Eos, Transactions, American Geophysical Union 77, 379.

Peyron, O., Goring, S., Dormoy, I, Kotthoff, U., Pross, J., Beaulieu, J.L. de, Drescher-Schneider, R., Vannière, B., Magny, M., in press. Holocene seasonality changes in central Mediterranean reconstructed from Lake Accesa and Tenaghi Philippon pollen sequences. The Holocene. doi:10.1177/0959683610384162.

Ravazzi, C., Rossignol-Strick, M., 1995. Vegetation change in a climatic cycle of early Pleistocene age in the Leffe Basin (Northern Italy). Palaeogeography, Palaeoclimatology, Palaeoecology 117, 105–122.

Ravazzi, C., Pini, R., Breda, M., Martinetto, E., Muttoni, G., Chiesa, S., Confortini, F., Egli, R., 2005. The lacustrine deposits of Fornaci di Ranica (late Early Pleistocene, Italian Pre-Alps): stratigraphy, palaeoenvironment and geological evolution. Quaternary International 13, 35–58.

Raymo, M.E., Nisancioglu, K.H., 2003. The 41 kyr world: Milankovitch's other unsolved mystery. Paleoceanography 18, 1–6.

Raymo, M.E., Lisiecki, L.E., Nisancioglu, K.H., 2006. Plio-Pleistocene ice volume, Antarctic climate, and the global $\delta^{18}O$ record. Science 313. doi:10.1126/science.1123296.

Real, V., Menochi, S., 2005. Distribution of the calcareous nannofossil Reticulofenestra asanoi within the Early–Middle Pleistocene transition in the Mediterranean Sea and Atlantic ocean: correlation with magneto- and oxygen isotope stratigraphy. In: Head, M.J., Gibbard, P.L. (Eds.), Early–Middle Pleistocene Transitions: The Land–Ocean Evidence, Geological Society, London, Special Publications, vol. 247, pp. 117–130.

Rial, J.A., 2004. Abrupt climate change: chaos and order at orbital and millennial scales. Global and Planetary Change 41, 95–109.

Rohais, S., Joannin, S., Colin, J.-P., Suc, J.-P., Guillocheau, F., Eschard, R., 2007. Age and environmental evolution of the syn-rift fill of the southern coast of the Gulf of Corinth (Greece). Bulletin de la Société géologique de France 178, 231–243.

Rohling, E.J., Hilgen, F.J., 1991. The eastern Mediterranean climate at times of sapropel formation: a review. Geologie en Mijnbouw 70, 253–264.

Rossignol-Strick, M., Paterne, M., 1999. A synthetic pollen record of the eastern Mediterranean sapropels of the last 1 Ma: implications for the time-scale and formation of sapropels. Marine Geology 153, 221–237.

Ruddiman, W.F., 2003. Orbital forcing ice volume and greenhouse gases. Quaternary Science Reviews 22, 1597–1629.

Ruddiman, W.F., McIntyre, A., 1984. Ice-age thermal response and climatic role of the surface North Atlantic Ocean (40°N to 63°N). Geological Society of American Bulletin 95, 381–396.

Russo Ermolli, E., 1994. Analyse pollinique de la succession lacustre Pléistocène du Vallo di Diano (Campanie, Italie). Annales de la Société géologique de Belgique 117, 333–354.

Sánchez-Goñi, M.F., Cacho, I., Turon, J.-L., Guiot, J., Sierro, F.J., Peypouquet, J.-P., Grimalt, J.O., Shackleton, N.J., 2002. Synchroneity between marine and terrestrial responses to millennial scale climatic variability during the last glacial period in the Mediterranean region. Climate Dynamics 19, 95–105.

Sánchez-Goñi, M.F., Turon, J.L., Eynaud, F., Gendreau, S., 2000. European climatic response to millennial-scale changes in the atmosphere–ocean system during the Lastglacial period. Quaternary Research 54, 394–403.

Sánchez-Goñi, M.F., Eynaud, F., Turon, J.L., Shackleton, N.J., 1999. High resolution palynological record off the Iberian margin: direct land–sea correlation for the Last Interglacial complex. Earth and Planetary Science Letters 171, 123–137.

Shackleton, N.J., Crowhurst, S., Weedon, G., Laskar, J., 1999. Astronomical calibration of Oligocene–Miocene time. Proceedings of the Royal Society of London A 357, 1907–1929.

Subally, D., Quézel, P., 2002. Glacial or interglacial: *Artemisia*, a plant indicator with dual responses. Review of Palaeobotany and Palynology 120, 123–130.

Subally, D., Bilodeau, G., Tamrat, E., Ferry, S., Debard, E., Hillaire-Marcel, C., 1999. Cyclic climatic records during the Olduvai Subchron (Uppermost Pliocene) on Zakynthos Island (Ionian Sea). Geobios 32, 793–803.

Suc, J.-P., 1984. Origin and evolution of the Mediterranean vegetation and climate in Europe. Nature 307, 429–432.

Suc, J.-P., Zagwijn, W.H., 1983. Plio-Pleistocene correlations between the northwestern Mediterranean region and northwestern Europe according to recent biostratigraphic and paleoclimatic data. Boreas 12, 153–166.

Suc, J.-P., Diniz, F., Leroy, S., Poumot, C., Bertini, A., Dupont, L., Clet, M., Bessais, E., Zheng, Z., Fauquette, S., Ferrier, J., 1995a. Zanclean (~Brunssumian) to early Piacenzian (~early–middle Reuverian) climate from 4° to 54° north latitude (West Africa, west Europe and west mediterranean areas). Mededelingen Rijks Geologische Dienst 52, 43–56.

Suc, J.-P., Bertini, A., Combourieu-Nebout, N., Diniz, F., Leroy, S., Russo-Ermolli, E., Zheng, Z., Bessais, E., Ferrier, J., 1995b. Structure of west mediterranean vegetation and climate since 5.3 Ma. Acta Zoological Cracoviense 38, 3–16.

Svenning, J.-C., 2003. Deterministic Plio-Pleistocene extinctions in the European cool-temperate tree flora. Ecology Letters 6, 646–653.

Tzedakis, P.C., 2007. Seven ambiguities in the Mediterranean palaeoenvironmental narrative. Quaternary Science Reviews 26, 2042–2066.

Tzedakis, P.C., Bennett, K.D., 1995. Interglacial vegetation succession: a view from southern Europe. Quaternary Science Reviews 14, 967–982.

Tzedakis, P.C., Roucoux, K.H., de Abreu, L., Shackleton, N.J., 2004. The duration of forest stages in Southern Europe and interglacial climate variability. Science 306, 2231–2235.

Tzedakis, P.C., Hooghiemstra, H., Pälike, H., 2006. The last 1.35 million years at Tenaghi Philippon: revised chronostratigraphy and long-term vegetation trends. Quaternary Science Reviews 25, 3416–3430.

Tzedakis, P.C., Pälike, H., Roucoux, K.H., de Abreu, L., 2009. Atmospheric methane, southern European vegetation and low-mid latitude links on orbital and millennial timescales. Earth and Planetary Science Letters 277, 307–317.

Von Grafenstein, R., Zahn, R., Tiedemann, R., Murat, A., 1999. Planktonic $\delta^{18}O$ records at sites 976 and 977, Alboran Sea: stratigraphy, forcing, and paleoceanographic implications. In: Zahn, R., Comas, M.C., Klaus, A., et al. (Eds.). Proceeding of the Ocean Drilling Program, Scientific Results, College Station. TX, pp. 469–479. vol. 161, Ocean Drilling Program.

Wijmstra, T.A., Smit, A., 1976. Palynology of the middle part (30–78 metres) of the 120 m deep section in northern Greece (Macedonia). Acta Botanica Neerl 25, 297–312.